Università di Roma Tor Vergata

Design and construction of RPC detectors

G. AIELLI

DRD1 GASEOUS DETECTORS SCHOOL

CERN, 03/12/2024

INFN Sezione di Roma Tor Vergata

Starting from the basics

- Any radiation detector exploits the physics of the interaction of radiation with matter
- the release of electromagnetic energy can be detected by a transducer
- In order to have a sufficient S/N i.e. to discriminate a signal above noise, the original signal, made of light or moving electrons undergoes amplification
- Amplification is obtained by a combination of the following ways:
  - By an amplifying physical process within the detector structure
  - By an electronic amplifier
- Any radiation detector couples a sample of matter as target, a transport mechanism and a transduction and amplification structures.
- Gaseous detector are characterized by using a gaseous target…
- The many types of gaseous detectors are differentiated by transport, transduction and amplification structures…

Quantum radiation → Material target → e.m. energy → Transport and internal amplification → Trans-duction → Electronic amplification

Why gaseous detectors?

- Technologically simpler than other solid state detectors, in facts they have been the first single particle detector “in real time” (Geiger counter 1908)
- Gas can be replaced so the target is not subject to deterioration
- They can be shaped easily in very different ways
- They can have very large and continuous targets (true also for liquid target detectors which are close relatives of gaseous detectors…)
- Their cost for unit surface or volume is low compared to other technologies
- For the characteristics above they have been used successfully in large spectrometers and tracking systems
- One iconic type the MWPC was awarded with Nobel Prize ☺ (Charpak 1992)

MicroMegas (MM)

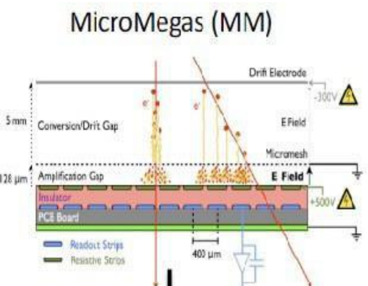

ATLAS new small wheels

GEM

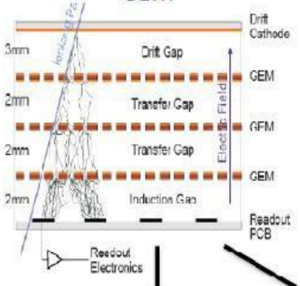

THGEM

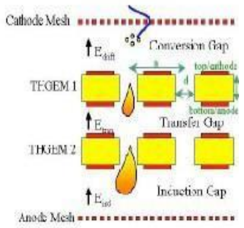

CMS GEM

ALICE TPC upgrade

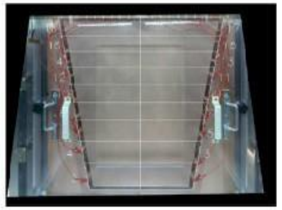

sMDT

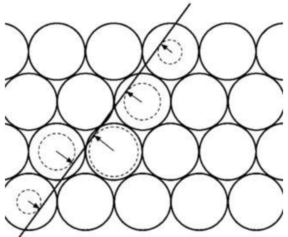

ATLAS Ph1 + Ph2 upgrade

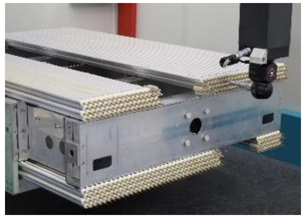

RPC

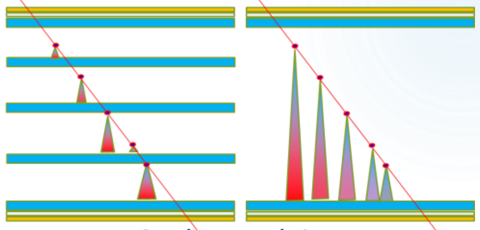

ATLAS Ph1 + Ph2 upgrade and CMS RE3/1 & RE4/1

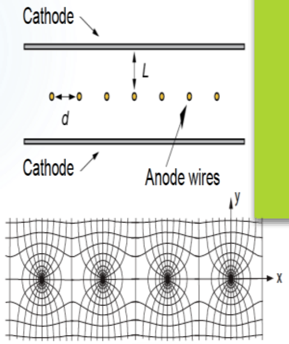

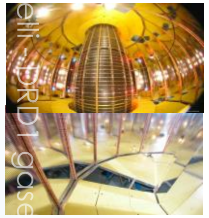

Muon detector technologies

AND NEW IDEAS

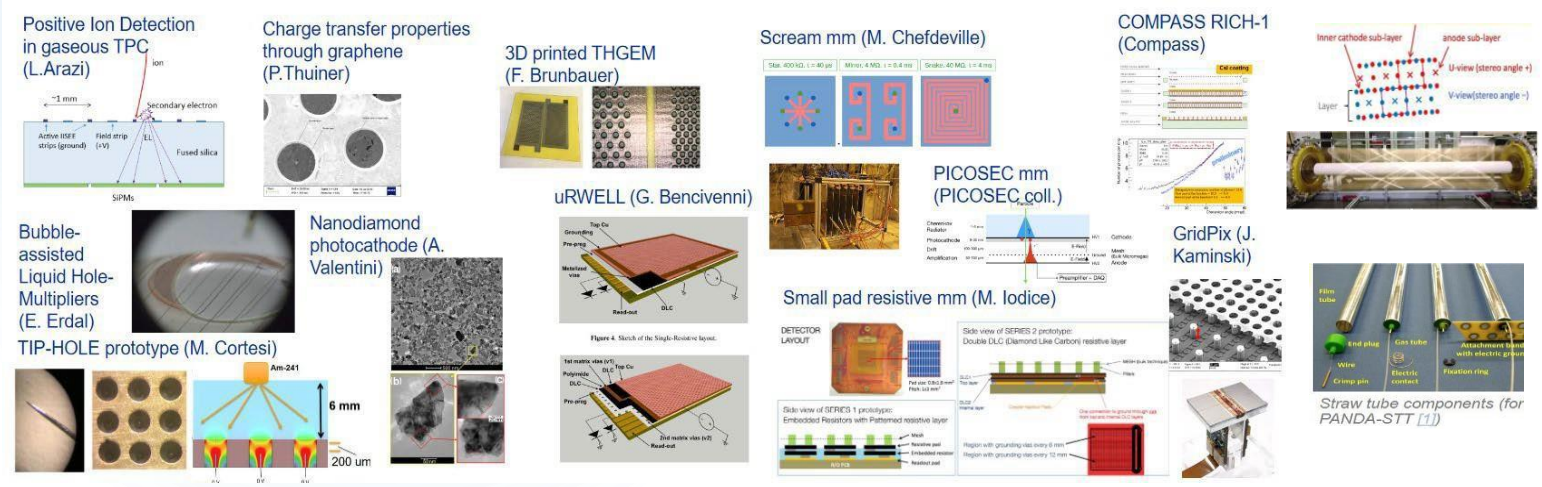

sRPC (Bencivenni

single gap semi-conductor
R. Cardarelli

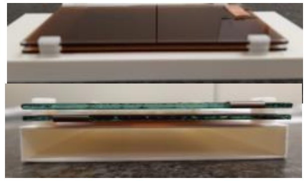

RCC Cardarelli

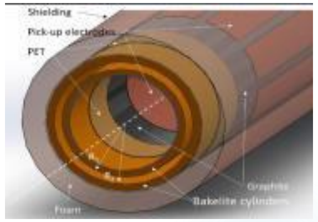

RPCs and within the main gaseous detector families

Basic principles of gaseous detectors

- All gaseous detectors designed for muons share the same base principle:
  - A gaseous target thick enough for a MIP to release a sufficient primary ionization
  - An electric field sufficiently strong to start an avalanche multiplication
  - A segmented pick-up electrode to readout the signal and extact a space-time information

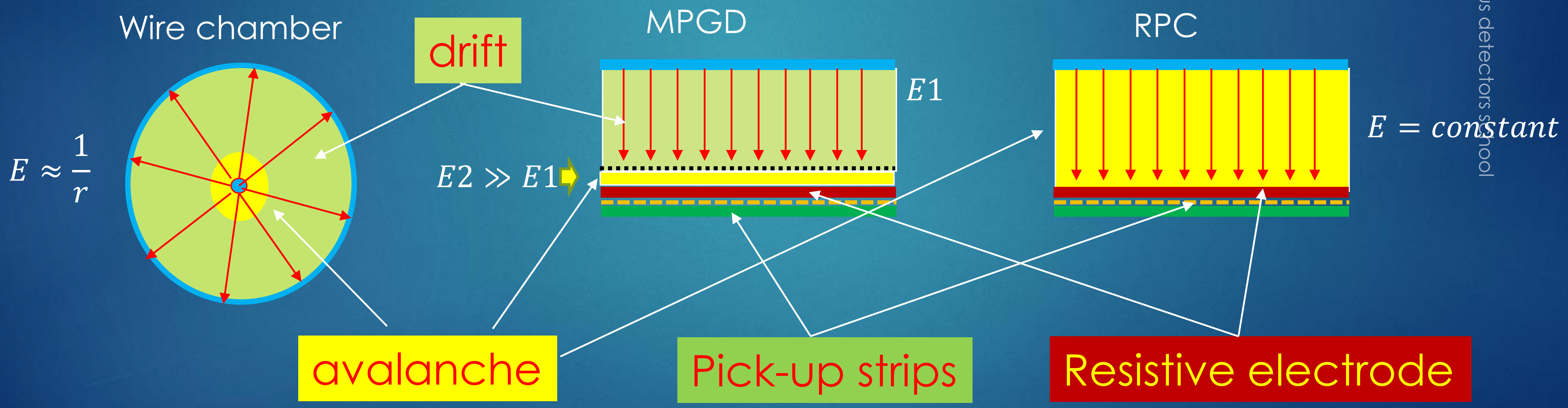

Resistive Plate chambers at a glance

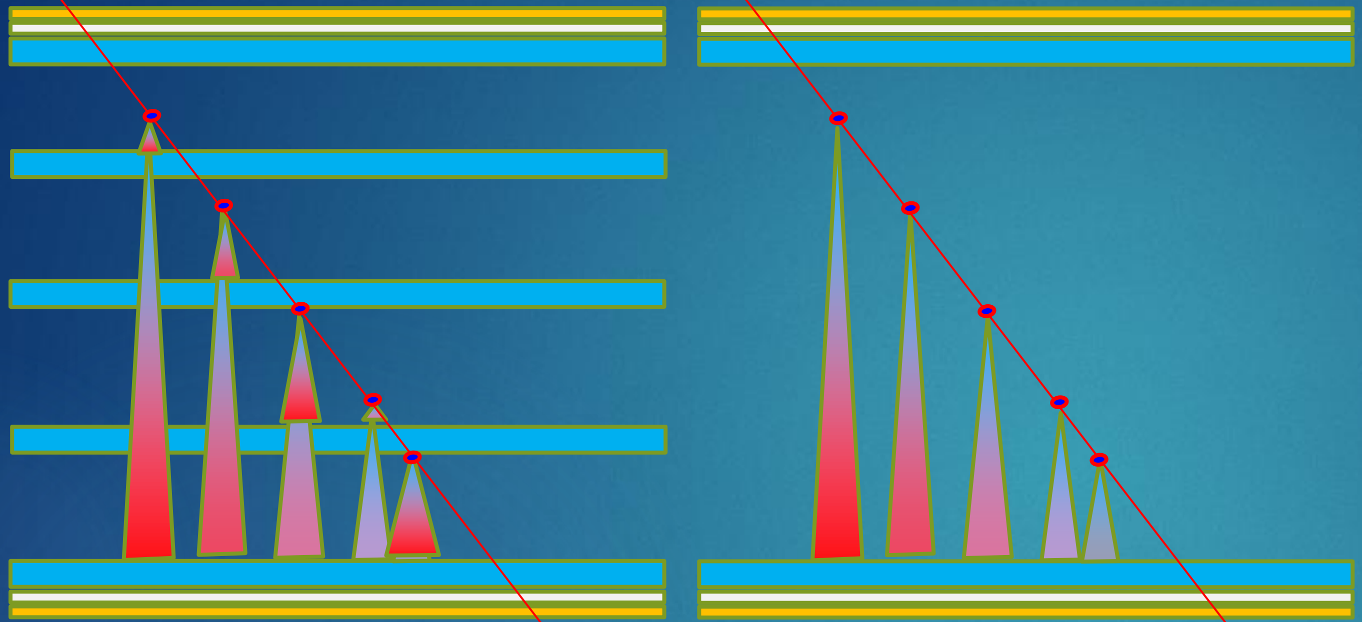

$$Q(V) = \ln\left(1 + e^{a(V-V_0)}\right)$$

$$Q(x) = \ln(1 + e^{\alpha x})$$

Integral logistic growth

G. Aielli et al NIM A 508 (2003) 6–13

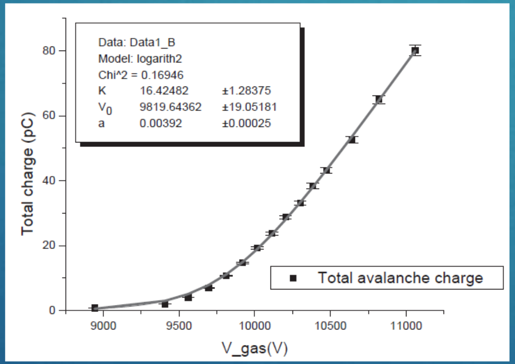

Common features

- high ρ electrodes → Spark less
- Uniform electrode → simple
- uniform field → prompt signal
- Working at atm. Pressure
- 0.1mm 2D localization
- Gas mixture

Feature	RPC vs	MRPC
# of gaps →	1 –	4 to tens
Gap size →	~1mm –	~ 0.1 mm
ρ(Ω cm) →	5×10^{10} –	5×10^{12}
Module size →	2 m^2 –	0.1 m^2
Hz/cm^2 →	10^4 –	5×10^2
σ_t →	300 ps –	50 ps
Electrode	HPL –	glass
Gas	R134A+ SF6 mix	

RPC Strength vs. weakness diagram

Continuous resistive electrode structure

→ Simple and robust construction

→ Spark free

→ Low cost

→ Easy to scale single module dimension to a few m^2 at constant unit cost and complexity

Gaseous target and multiplication coincide

→ prompt avalanche → high time resolution and efficiency

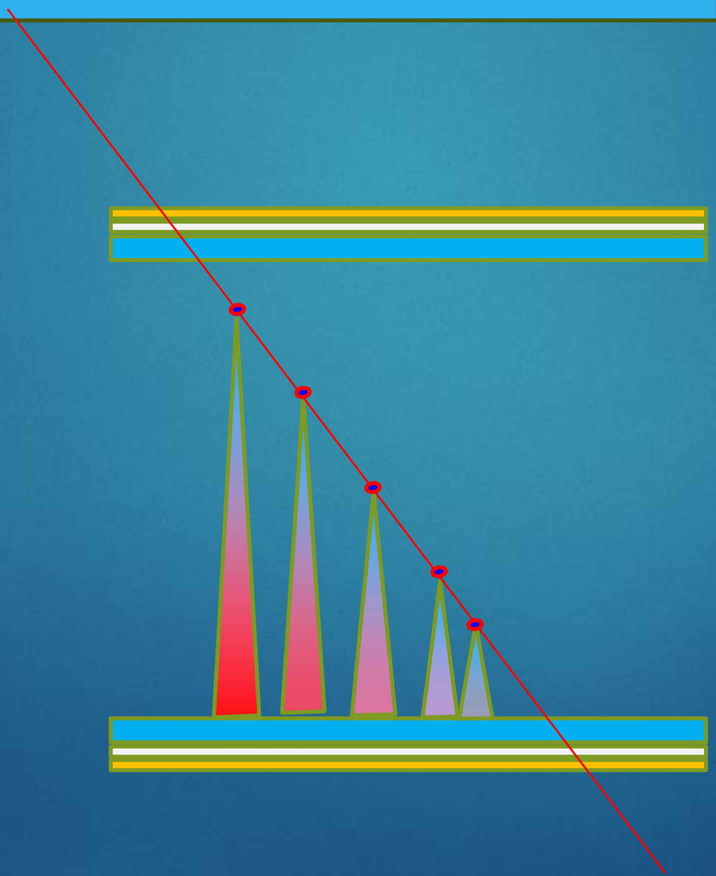

→

- Cluster number and depth
- Cluster size fluctuations
- Multiplication fluctuations

→ Very wide avalanche charge range and high <Q>

→

- High operating current
- transition to streamer
- limitation to rate capability

→

Implications:

- challenging electronics
- “low” resistivity electrodes
- electronegative gases

State of the art of classic rpcs

- (some of)Present and recent past Application at colliders

- PRESENT AND RECENT PAST COSMIC RAYS AND UNDERGROUND

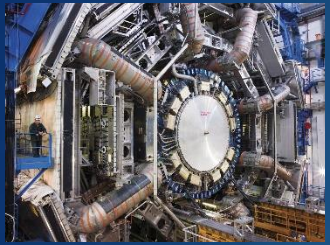

ATLAS
LHC 7000 m^2
HL-LHC1400 m^2
Tracking trigger

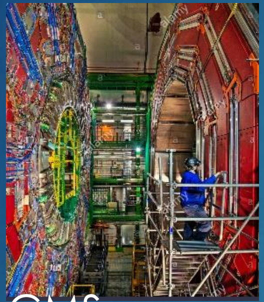

CMS
LHC 4000 m^2
HL-LHC1000 m^2
Tracking trigger

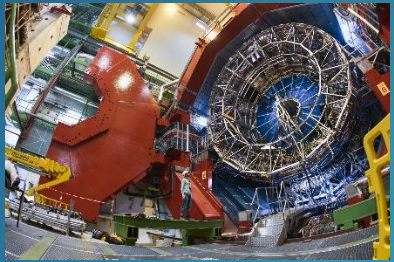

ALICE
LHC 144 m^2
HL-LHC new RPCs
Tracking trigger

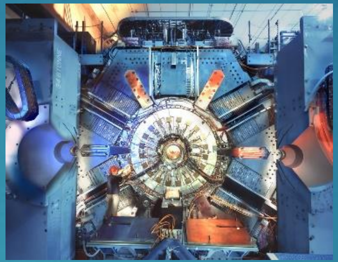

BaBar
SLAC 2000 m^2
Instrum. iron
μ identifier

OPERA
CERN ν beam
3200 m^2
Instrum. iron
μ spectrometer

ARGO Ybj
CR exp. 7000 m^2
4600 m altitude
3D reconstruct.

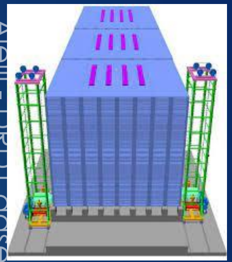

INO (staged)
ν observatory
150000 m^2
Instrum. Iron

- ACTIVE PROPOSALS FOR FUTURE EXPERIMENTS USING PRESENT TECHNOLOGY

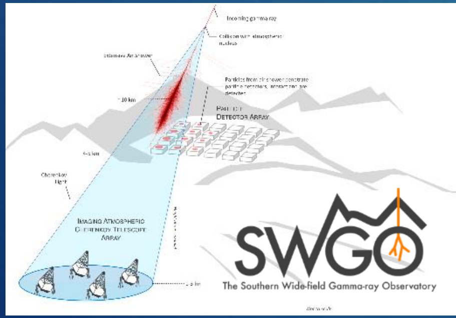

SWGO - STACEX
CR exp. 22500 m^2
5000 m altitude
3D reconstruct. +
Cherenkov

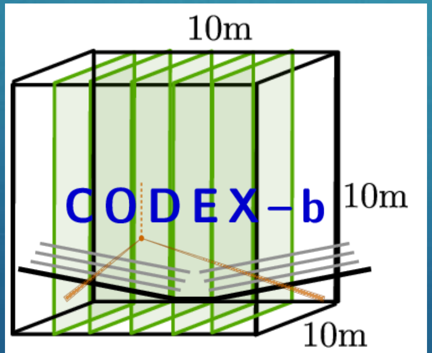

CODEX-B
HL-LHC. 3000 m^2
Search for DM
Sealed tracking volume

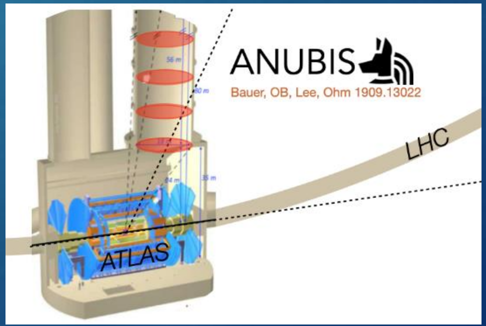

ANUBIS
HL-LHC. 5500 m^2
Search for DM
Sealed tracking volume

State of the art of mrpcs

- Applications in current and future HEP and NP experiments
- CBM expected rate up to 10–25 kHz/cm2 in the central region

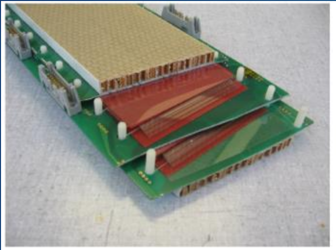

ALICE@CERN
10.1016/S0168-9002(01)01753-3

Mostly used as extensive (up to ~ 200 m^2) TOF systems with time resolution up to 50 ps

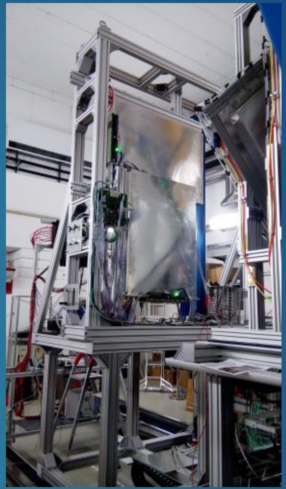

FD-HADES@GSI

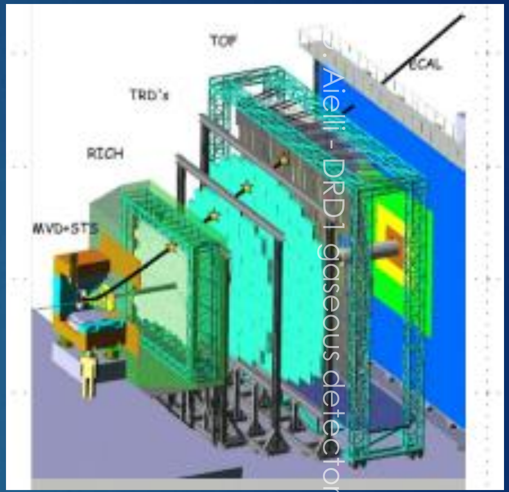

CBM@FAIR 10.1088/1748-0221/14/09/C09020

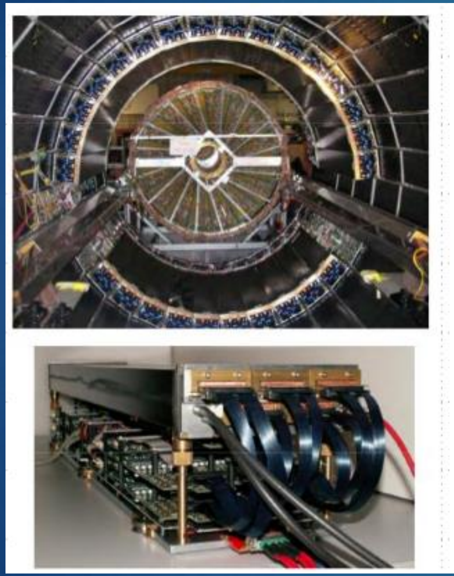

FOPI@GSI
10.1016/j.nima.2004.07.002

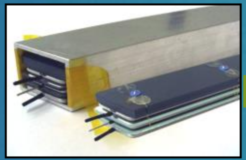

HADES@GSI
10.1016/j.nima.2008.12.090

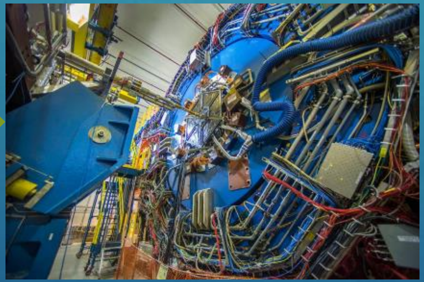

START@RHIC 10.1016/j.nima.2010.07.086

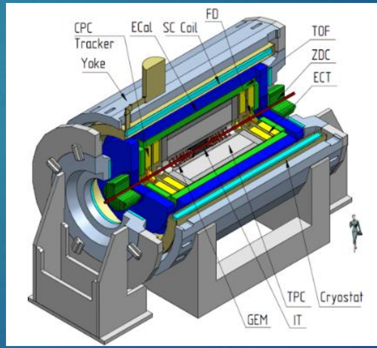

MPD, BM@N at NICA facility
10.1051/epjconf/201817112001

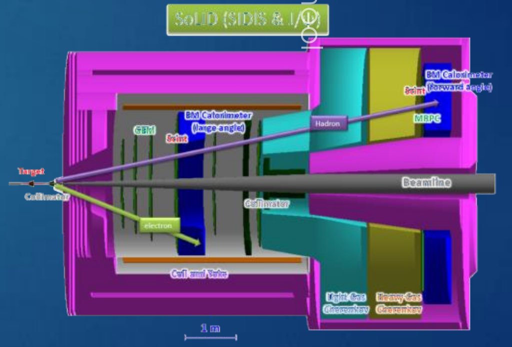

SoLID (Jefferson Labs)
arXiv:1409.7741v1 [nucl-ex] 26 Sep 2014

Can be found also application in muon tomography of large geological structures and PET

RPC technical challenges vs. construction

Overview of the RPC technology

- As you may have noticed, RPCs look easy to build also with limited technology level
- You may have had the you-can-do-it-yourself impression ☺
- This impression comes from the simple structure and absence of micromachined parts, simple physics laws are apparently in place to govern the signal development
- Actually, a lot of electro-chemistry in it as we will see.
- The physics laws governing an RPCs are not so simple, often non-linear
- We will go through the main features of RPC functioning and the way to obtain them
- The initial idea of simplicity will be probably partially change…

Resistive Plate Chamber

- One of the primary features of the RPC is the resistive electrodes
- Requirements:
  - Uniformity: a continuous piece of material industrially produced
  - a volume resistivity ranging in between 10^8 - 10^12 Ohm cm
  - Relative Dielectric constant around 5-7
  - The resistivity should be stable in the detector lifetime → carriers non depleted
  - A continuous resistive layer is needed to localize the discharge, but it limits the rate capability: in presence of a uniform background, the voltage drop is $\Delta V = IR = \langle Q \rangle (pC) \cdot f(Hz) \cdot \rho(Ohm\ cm) * {}^{d}/_{S}\,(cm^{-1})$

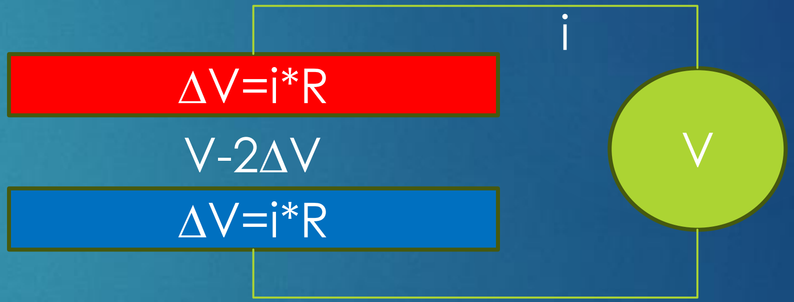

  - Having d=1 mm of electrode thickness and $\rho = 10^{10}(Ohm\ cm)$, a current of 10 μA given by a 1 MHz/m^2 of MIPS producing in average 10 pC of avalanche charge, would produce a field of 1 V/mm in the electrode
  - To be compared to the typical applied field of about 5000 V/mm
- The field in the electrode should be "small" to have most of the field on the gas. Vice versa this limits the rate capability (through the voltage drop) and the longevity by deplating the electrode

Resistive Plate Construction

- Such resistivity range is not common for large plates of materials. Most commonly used material:
  - High Pressure Laminate ranging between 10^9 and 10^12 Ohm cm
    - Low cost per unit surface
    - High mechanical stability
    - Carriers are water ions (internal water concentration goes in equilibrium with the environment)
    - The plate is in between 1 and 2 mm
  - It is produced by pressing together at high temperature a core of several layers of kraft paper impregnated with phenolic resin, finished externally with melamine impregnated paper.
  - The hot press produces the resin polymerization
  - The melamine provides a harder surface and carries most of the resistivity

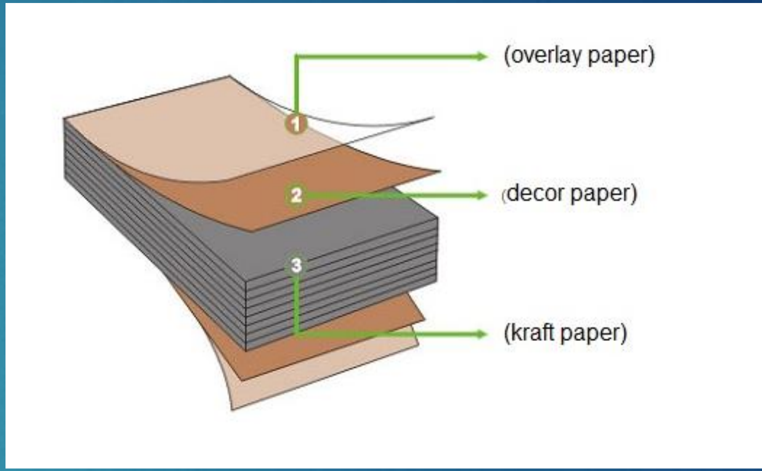

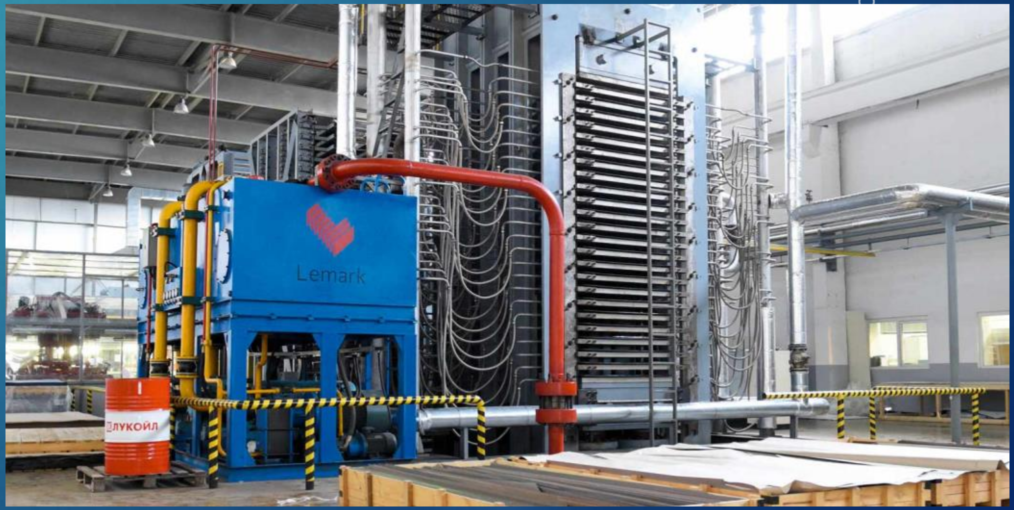

Resistive Plate Endurance

- HPL is hygroscopic
- It behaves as porous water container setting surrounding environment to an equilibrium point around 40% RH

- HPL ELECTRICAL CONDUCTION IS MEDIATED BY WATER IONS
- A CONSTANT AVAILABILITY OF WATER MOLECULES AT THE ELECTRODE ANODIC FACE, GUARANTEES A STABLE CONDUCTIVITY

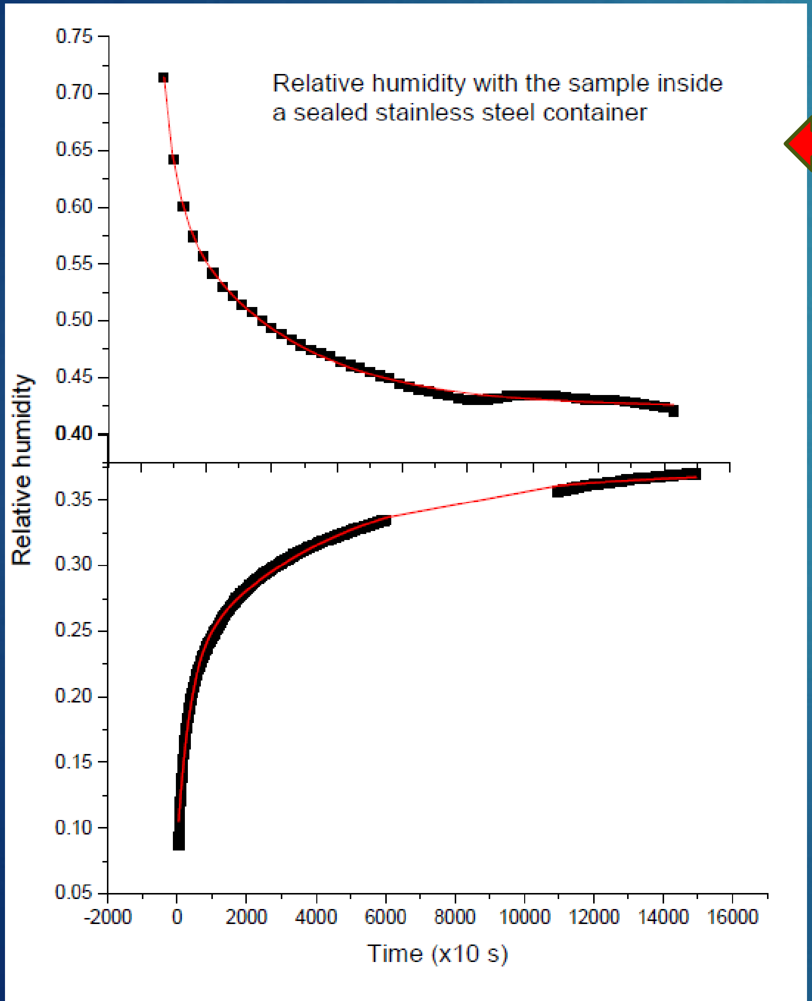

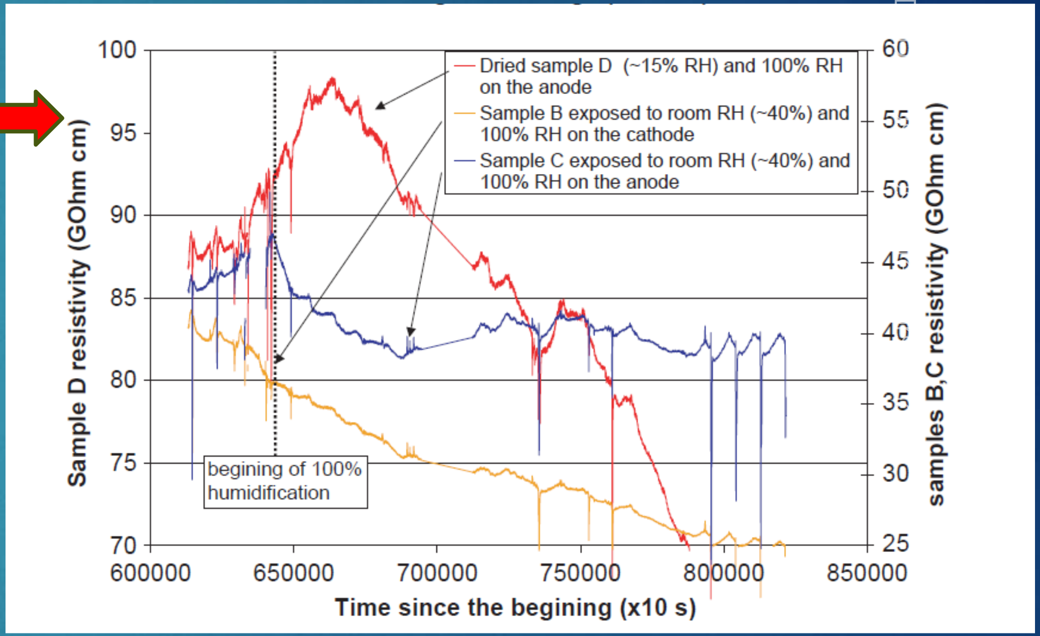

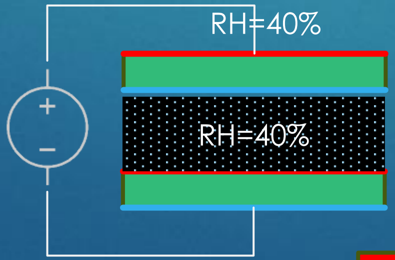

- TO EXPOSE THE ANODE SIDE OF EACH RPC ELECTRODE, BOTH ENVIRONMENT AND GAS MUST BE KEPT AT CONSTANT RH (AROUND 40%)

Resistive Plate Construction

- The other commonly used material is glass
- **Soda-lime glass**: The typical resistivity is 10^{12} Ω·
  - This is the most commonly used type of glass in RPC detectors.
  - It provides a good combination of:
    - **Surface resistivity uniformity**, which is crucial for the consistent operation of the chamber.
    - **Mechanical stability**, to maintain the flatness of the plates.
  - It is relatively inexpensive and easy to process.
- Drawbacks are the weight, fragility, and high resistivity, making it suitable for cosmic rays experiments.
- Must be operated with a dry gas if in presence of fluorinated gases, since glass is very sensitive to HF
- Advantage: more rigid and higher mechanical precision than HPL → suitable for very thin electrodes
- It is the election material for the micro-multi gap RPCs where the electrode thickness is of the order of 0.2 mm

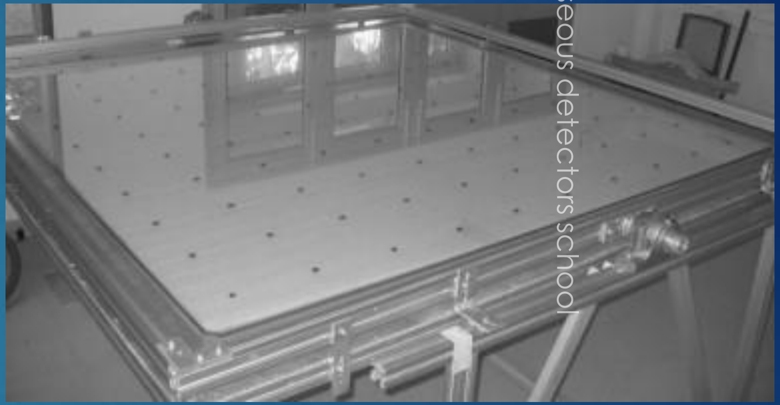

Resistive Plate alternatives

- MRPC → EXTREME EXPLOITATION OF THE DETECTOR GEOMETRY TO EXTRACT THE MOST OF <Q>
  - E.G. ALICE: 10 GAS GAPS OF 0.25MM WITH 0.4 MM ELECTRODES
- MAIN LIMITATION → THIN FLOAT GLASS LIMITED TO < 1 KHZ/CM² DUE TO $\rho \sim 10^{12}$ Ω/CM.
- NEW MATERIALS WITH LOW RESISTIVITY (DOWN TO 10^{9-10} Ω/CM) →(CERAMICS, PLASTICS, GLASS,…)

(10.1016/J.NIMA.2006.12.027, 10.1016/J.NIMA.2010.08.076, 10.1016/J.NIMA.2020.163483, 10.1088/1748-0221/14/09/C09007, HTTP://CDS.CERN.CH/RECORD/2319919

  - CARRIER DEPLETION EFFECTS → R&D NEEDED
  - MATERIAL NON-HOMOGENEITIES FOR LARGE SIZES
  - THINNING ELECTRODES STILL POSSIBLE.
  - FORCED (NO DIFFUSION) GAS DISTRIBUTION
- LARGE MARGIN ACHIEVABLE BY LOWERING < Q >

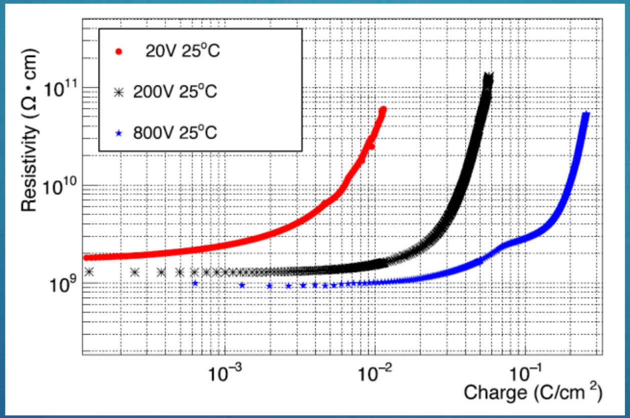

A new device: single gap semi-conductor RPC [electronic carriers can not be depleted]

- Counting rate > 40 kHz/cm²
- 0.6 mm GaAs electrodes
- Resistivity 1.4×10^8 Ωcm
- 1 MHz/cm² seems possible
- Active area 6.25 cm²
- 10.1088/1748-0221/15/12/C12004

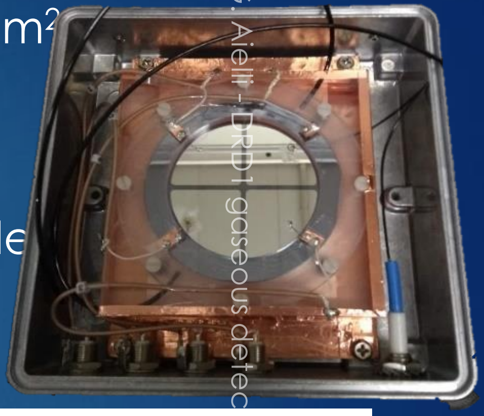

G. Aielli - DRD1 gaseous detec

FFC TARGET → improve by a further order of magnitude by lowering R

Resistive Plate Chamber - surface

- The other characterizing feature is the uniform and strong electric field → plate configuration.
- The advantage is the production of a signal without delay and the naturally achieved 3D+t localization of the hit with high space-time resolution, on large surfaces.
- The disadvantage is that it is difficult to maintain such a configuration in a stable way, due to the spontaneous electron emission from the electrode surface, by edge effect (cold electron extraction)
- The resistive plate prevents the lateral propagation of the discharge, but the spontaneous discharges may overwhelm the detector response
  - This is affecting in particular HPL electrodes → the surface finishing is determined mechanically determined by the press iron plate finishing. Moreover HPL is a multilayer polymer. The expected local roughness distribution is wide, with an average of the order of several μm
  - Glass is a liquid so naturally smooth (roughness from 10 to 100 nm)
  - silicon is a crystal cut along a specific layer (roughness of the order of a few nm)

Resistive Plate Chamber – HPL case

- HPL was the first material used for RPCs
- A very special procedure has been invented to have a glass-like finishing
- Varnishing the internal surface with a few μm layer of linseed oil
  - Linseed oil was the "secret" of the Flemish painters in the XVI century…
  - Upon polymerization, linseed oil forms a hard and glossy surface, and its resistivity is similar to the one of HPL
  - Oiling is applied by slowly filling and emptying gas volumes vertically held, with a mixture of linseed oil and heptane, and subsequently stimulating the polymerization (oxygen driven) by flushing the gas volumes with clean air.
  - The polymerization lasts a few days and is performed at T> 35 °C

First plateau using linseed oil (by R. Cardarelli)

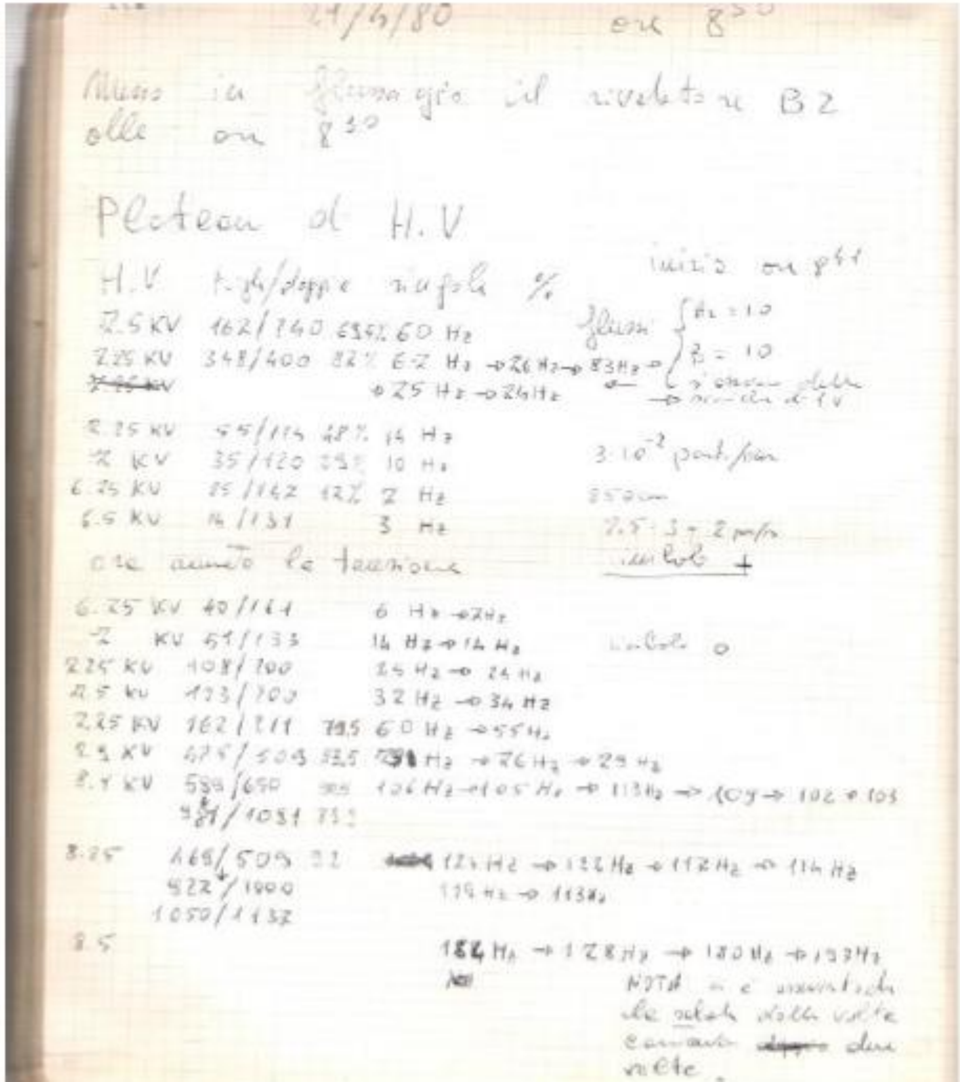

Resistive Plate – ohmic contact

- The external face of the electrodes are treated with a graphite layer with a surface resistivity << of the HPL one
- This represents an ohmic contact and has the function of distributing the electric potential uniformly on the surface
- Its surface resistivity is of the order of 100 kOhm/□
  - Typical τ=RC=10 pF*100 kOhm = 10^{-6} s
  - Sufficiently slow to be transparent to the prompt avalanche signal ($\tau \approx 1ns$)
- The graphite contact is progressively damaged by the electro-chemical reactions, using a thick layer, we demonstrate that the system can withstand the full ATLS program

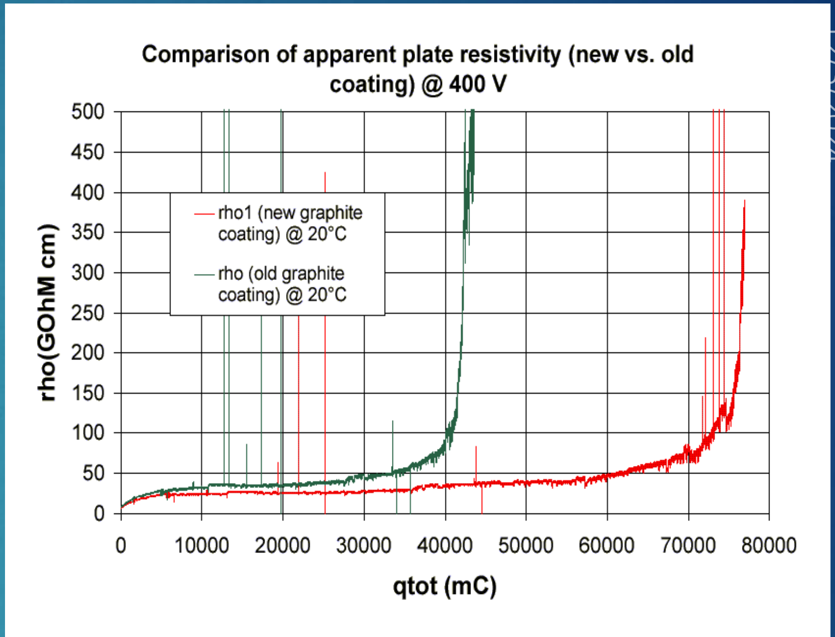

Choice of the graphite: it is possible to obtain the same resistance per square with different amounts of graphite per unit surface, by adding a resin as a filler in between the graphite grains. Such a thicker structure is more resilient to chemical damage

Resistive Plate – electrode thickness

- The electrode thickness should be idealistically as thin as possible since the signal induction is given by the weighting field through the Ramo theorem as:
- $$i(t) = \frac{E_w}{V_w} v e_0 N(t)$$ Where $\frac{E_w}{V_w} = \frac{1}{\frac{2b}{\varepsilon} + d}$
- Since ε is about 7 the electrode thickness contribution is reduced:
- Example: b=1mm d=2mm → 77% we have a reduction of 23% for the signal with respect to a zero thickness electrode
- On the other side a too thin electrode becomes mechanically unstable due to the electrical force in between the electrodes
- Practical ranges are in between 1.4 and 2 mm

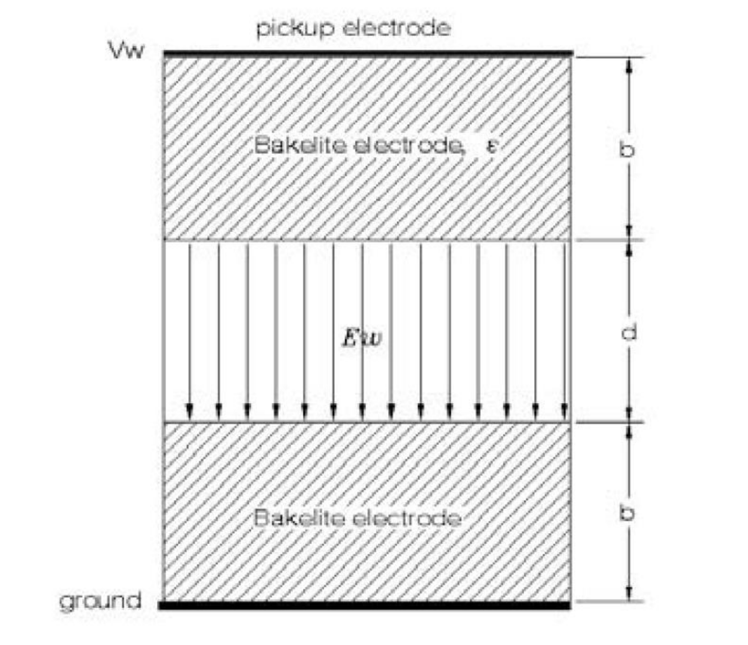

Resistive Plate Chamber gas gap

- We consider a chamber as a closed and defined gas volume
- The electrodes are kept at constant distance by a set of spacers placed at a distance such that the catenary profile in between 2 spacers is <<< of the gas gap
- Having a more or less thin gas gap has pros and cons

- Pro:
  - higher time resolution
  - Lower applied voltage
  - The same charge, produces a higher saturation of the field
  - Higher space resolution
- Cons:
  - Less statistics of primaries → the bottom line is $P(0) = e^{-\frac{d}{\lambda}} \leq Eff$ where λ is the ionization mean free path
  - Higher mechanical sensitivity
  - Higher FE amplifier performance

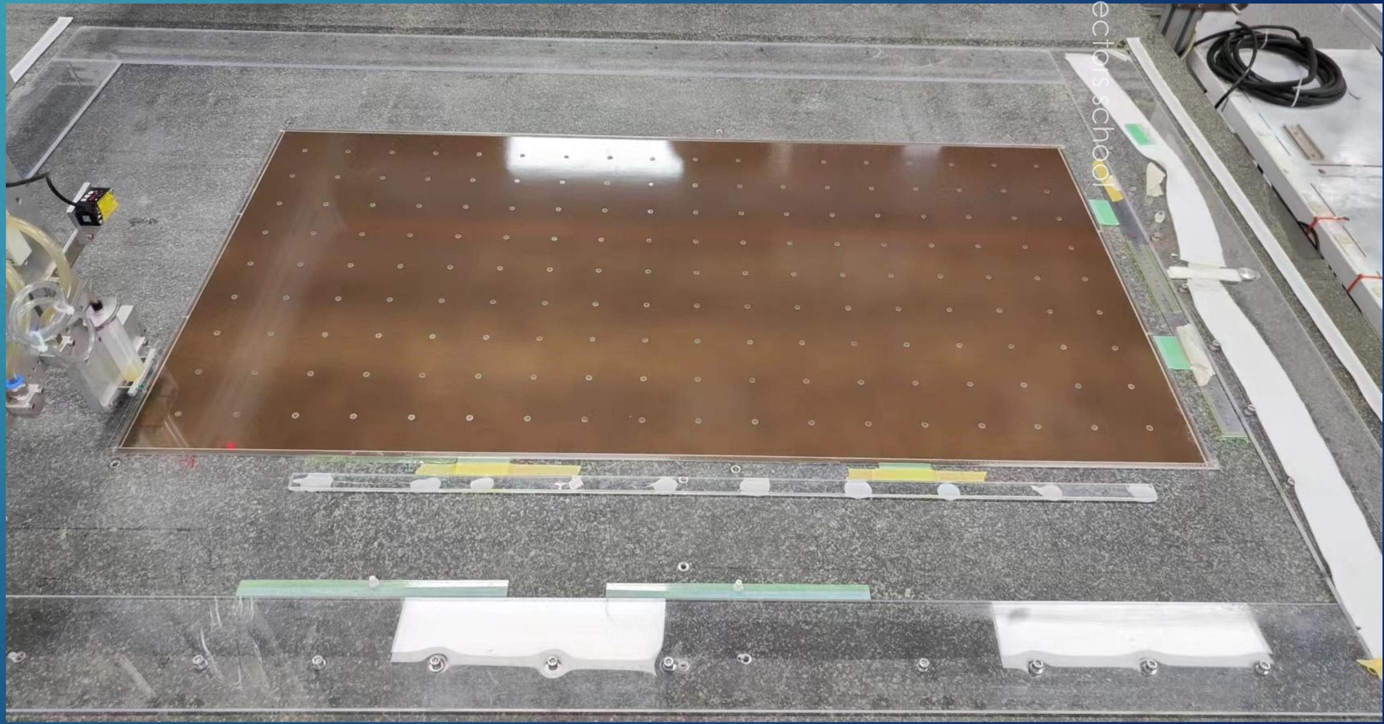

Resistive Plate Chamber avalanche

- Primary ionization points follow the Poisson distribution

$$f(k;\lambda)=\Pr(X{=}k)=\frac{\lambda^k e^{-\lambda}}{k!},$$

- Their number depends essentially by the gas electron density
- The amount of energy released in each point follows the Landau distribution
- It doesn't have a defined average value and the integral is infinite
- The first limitation comes from the primary particle energy…
- If the avalanche was developing just exponentially, one applies the superposition principle, and the total charge is a sum of exponentials where each multiplicative constant is given by Landau.
- Luckily, as soon as the number of electrons increases, the avalanche growth from exponential becomes linear

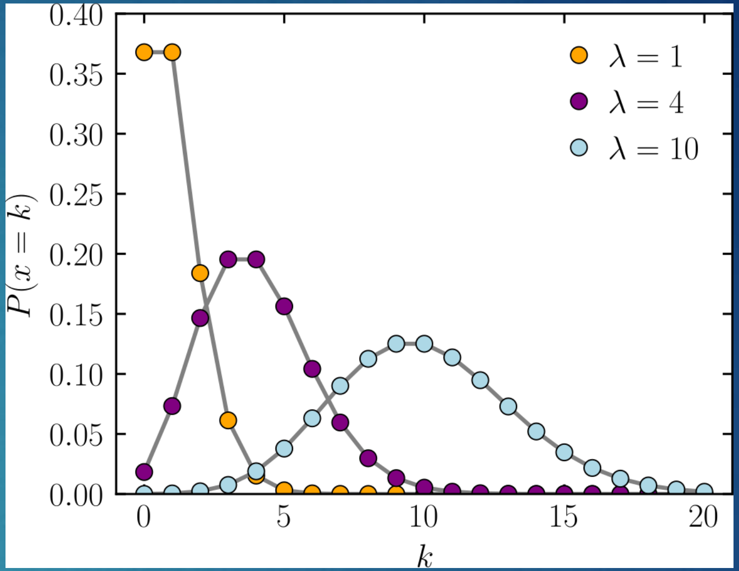

The experimentally observed growth of the avalanche charge recalls the Logistic function introduced firstly in 1845 by Verhulst [8] to describe the growth of a biological population, that tend to become stationary in presence of a limited flow of food resources due to the fact that the number of individuals able to reproduce become constant.

In our case the experimental data on the total charge can be compared with the integral of the logistic function, accounting for the total population: the multiplying (active) electrons and the spectator electrons

$$Q(V)=K\ln(1+e^{a(V-V_0)})$$

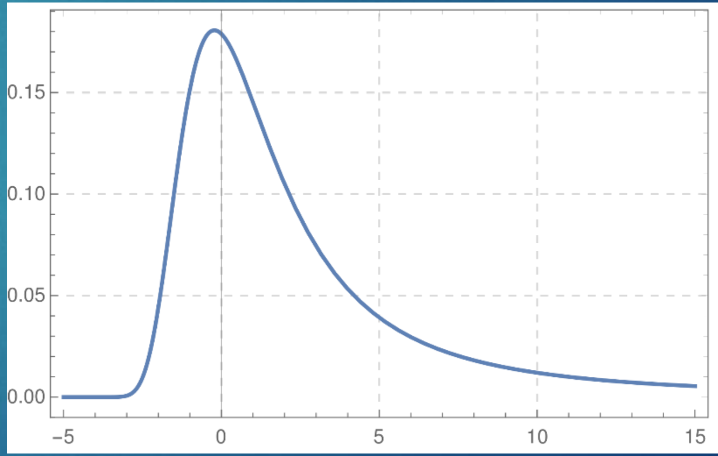

Resistive Plate Chamber vs. amplifier

State of the art FE →
noise = 4000 e- RMS

Threshold on the injected signal →
20000 e- RMS

Assuming to lose a factor 40 on the induction →
avalanche geometry x Ramo x readout strip

8*10^5 electrons for the minimum detectable signal

Rough assumptions on charge distribution for saturated avalanches
- mode ≈ average ≈ 3 x minimum
- Average ≈ 15 x minimum

- Ideal case~ 0.4 pC
- 7.5 times better of the single gap state of the art (3 pC real case)

Worsening of FE performance proportionally reflects on <Q>
Correlation between narrower gas gap and FE threshold

- Two parameters are important to determine the maximum rate capability:
  - FE threshold
  - Asymmetry of the charge distribution
  - A perfectly saturated avalanche would produce a gaussian distribution

Gas gap optimization parameters:
- As small as possible to achieve saturation with proportionally fewer electrons → 0.1 mm
- Deep saturation also increases the induction efficiency
- Below 1 mm gas gap P(0) is not negligible, and part of the advantage is lost due to the necessity of amplifying very unfavorable primary electrons (placed close to the anode) by increasing the electric field
- Therefore, the MRPC use many tiny gas gaps

Resistive Plate Chamber S/N

- The RPC is typically a very large structure (a few m^2)
- A signal or a disturbance takes a few tens of ns to travel end to end
- The amplifier and discriminator produce typically a fast transient resulting an in very high instantaneous current injected on the ground. This under any aspect is seen as a signal if the ground scheme is not able to dissipate or compensate it
- There are the following types of noise:
  - Self-induced current coupled noise (diaphonicity), the one above
  - External noise coming from the environment, this can be dominant if the faraday cage is not strong enough
  - Intrinsic electronic noise, of the order od a few hundred to a few thousand of electrons
  - The first 2 are generally dominant unless the grounding is able to suppress them

Different RPC layout brought to different operative thresholds:

- Legacy ATLAS – 20 fC one 2 mm gas gap
- Legacy CMS – 40 fC two 2 mm gas gaps
- Upgrade ATLAS 3 fC one 1 mm gas gap
- Upgrade CMS 40 fC two 1.4 mm gas gaps

1.3) iRPC readout

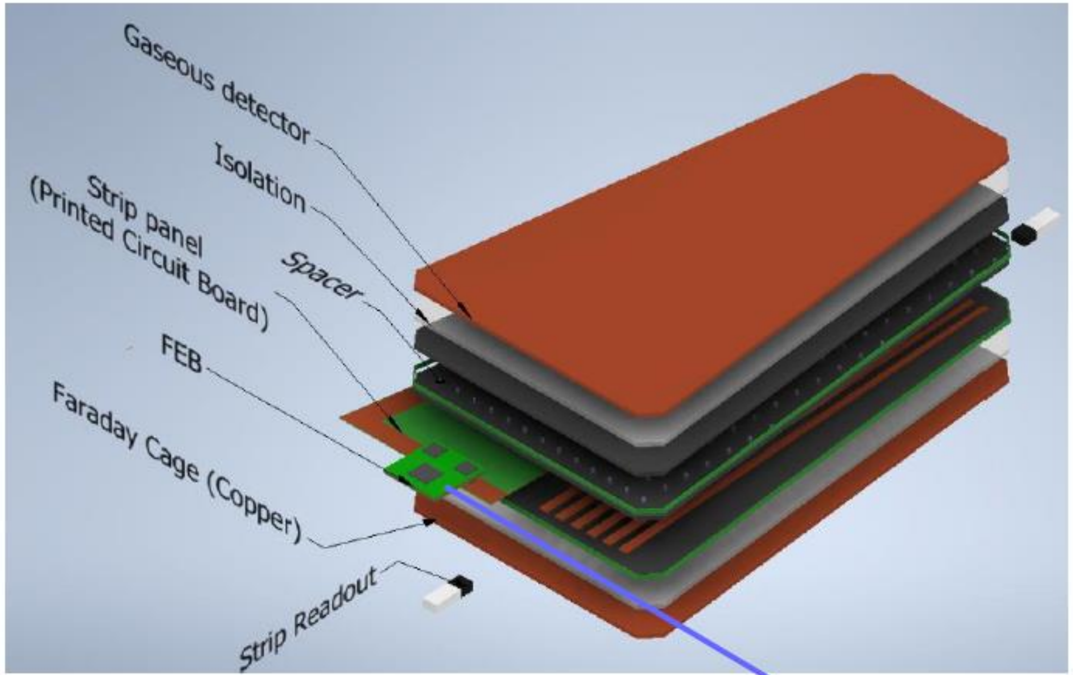

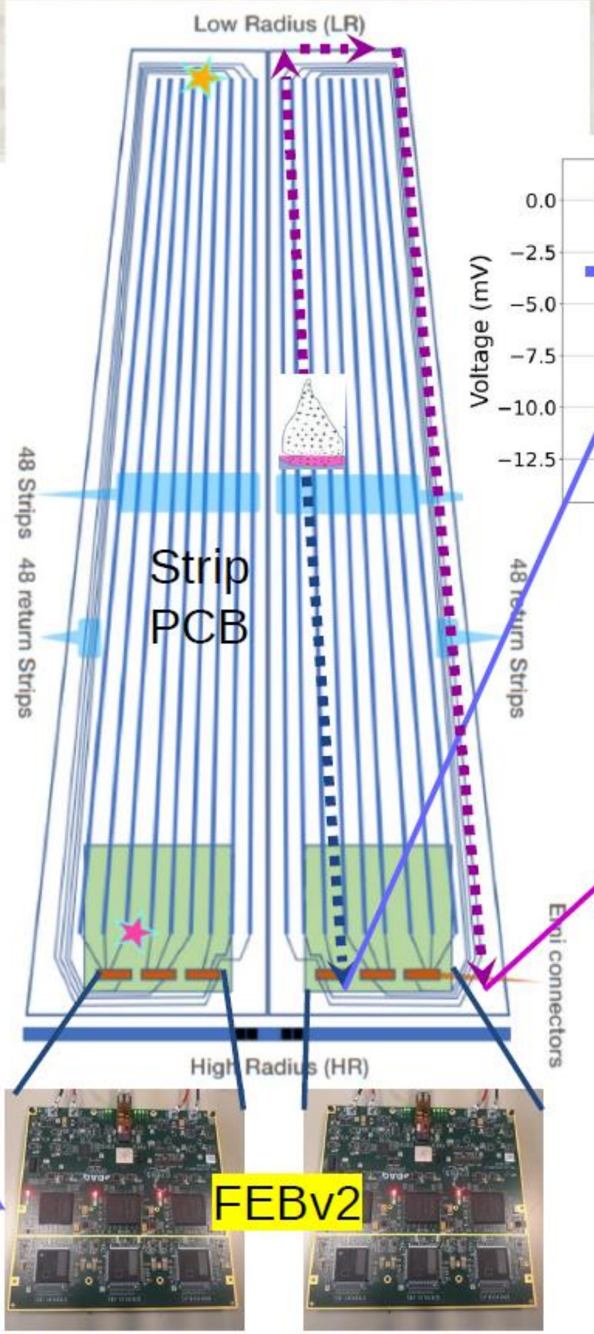

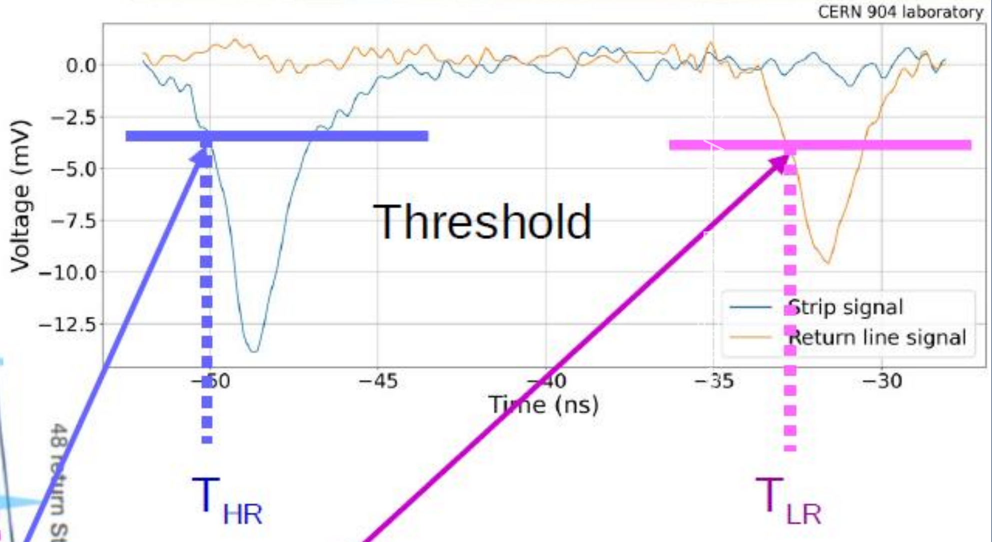

- Strip pitch : 0.5 – 1 cm
- Double sided readout of long strips using timing to localise the signal position

$\Delta T = T_{HR} - T_{LR}$

$\sigma_{\Delta T} \sim 150$ ps $\rightarrow \sigma_{\eta} \sim 1.5$ cm

M. Gouzevitch: iRPC front-end board readout electronics. RPC2024

BI RPC Challenges – Physical encumbrance & new detector structure

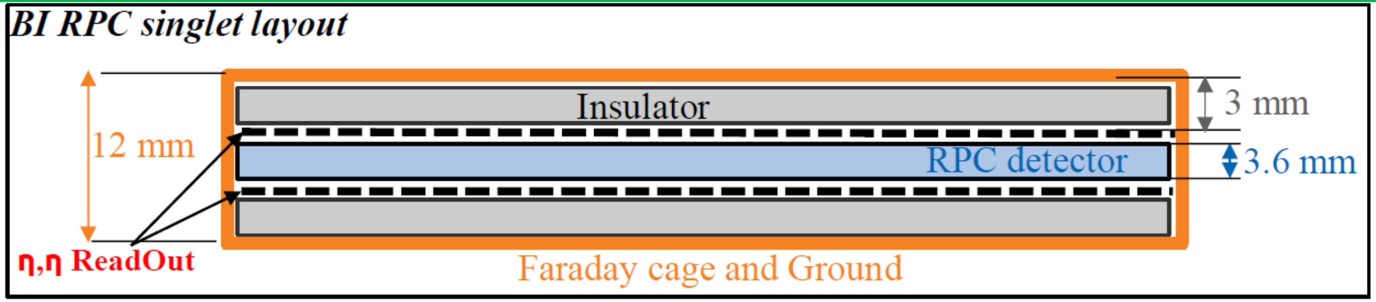

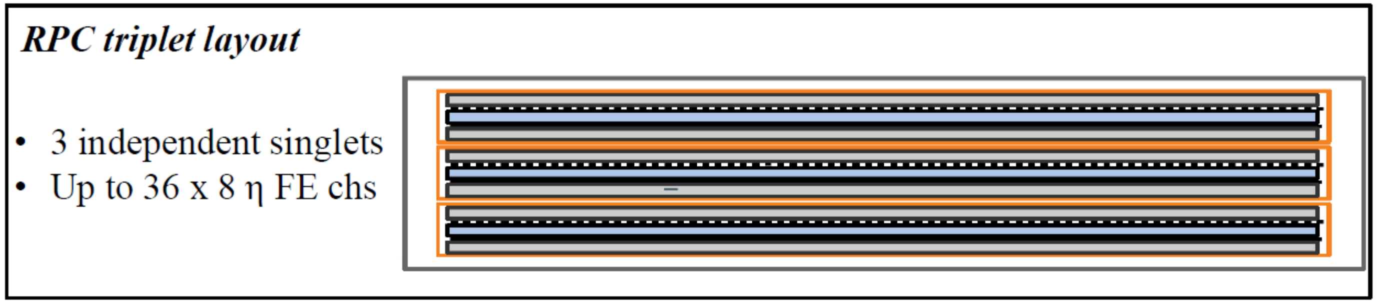

	ATLAS RPC currently installed	ATLAS New generation RPC
Detector	Mono gas gap	Mono gas gap
Gas Gap width	2 mm	1 mm
Electrode Thickness	1.8 mm	1.3 mm
Gas Mixture	95% TFE, 4.7% i-C4H10, 0.3% SF6	95% TFE, 4.7% i-C4H10, 0.3% SF6
Time Resolution	1 ns	0.4 ns

The available space in the ATLAS muon-spectrometer inner barrel implies mainly:

- Few centimeters space (in the orthogonal direction wrt the beam) for the full detector placement along with most of its services
- Some fully inaccessible zones

→ **Detector and services structures re-design**

- No room for the electronics on the detector phi side due to geometrical factors and impossibility to overlap the detectors

→ **Parallel strips readout** (second coordinate measured with the time arrival difference at the detector edges)

The time resolution < 100 ps of the TDC embedded in the FE allows the reconstruction of the second coordinate with 1 cm space resolution.

BIS singlets assembly (Training @ BB5)

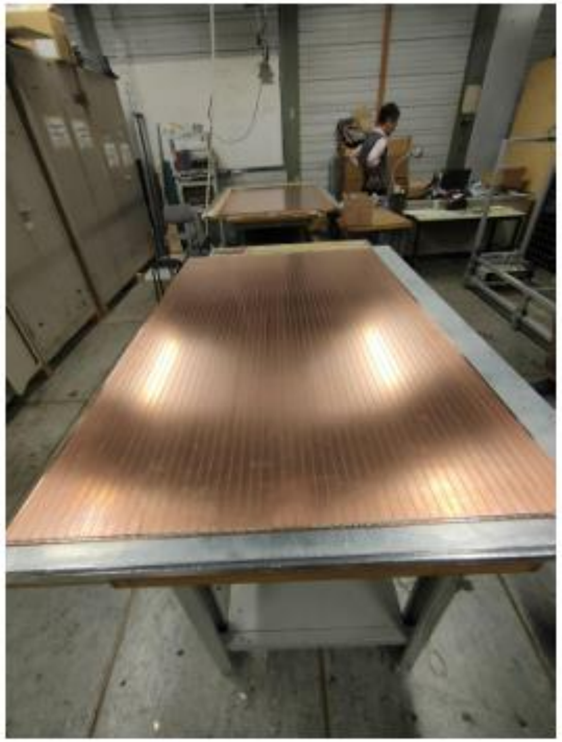

Step1:
Put the readout pannel in the table with strip pannel on the top

Step2:
Put the gas gap on the top of the readout pannel

Step3:
Put another readout pannel on the top of the gas gap

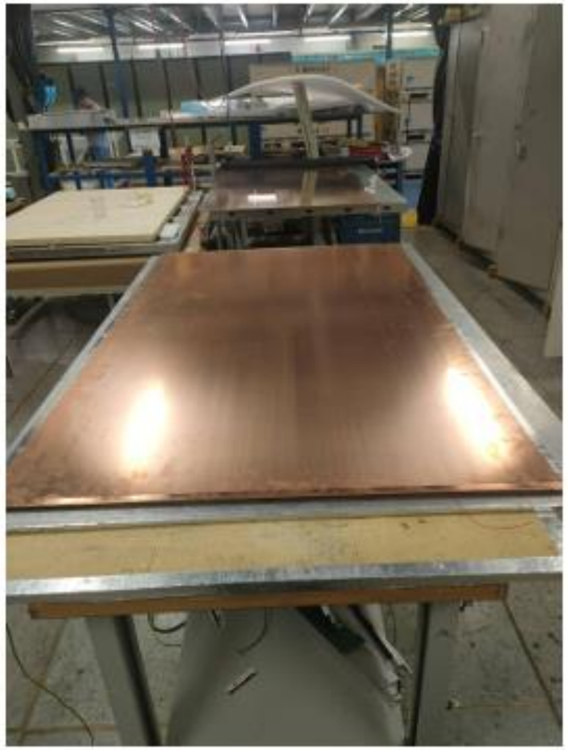

Step4:
Use the Aluminium tape to fix those three layers to form the singlet

Focus on the singlet structure and readout scheme

- The singlet structure is mean to integrate the FE electronics within the detector
- It allows to implement an adequate grounding scheme to neutralize the self-induced noise
- The signal is amplified as close as possible to the source (maximum S/N)
- If possible, the signal is digitized and transmitted out not as a pulse but as data
- More details tomorrow in Roberto presentation about electronics

RPC construction sites

Summary of the gas gaps production sites

Classic RPCs – main sites (known to me)

- GTE (Colli – FR) it is the historical site where most of the classic RPCs have been built (ATLAS-CMS-ARGO-OPERA-BaBar etc)
- Production in Korea for CMS (see next slides)
- Production at MPI for ATLAS (new entry)
- Production at USTC (new entry)

MRPCs

- Smaller productions – lab driven

Production of iRPC electrodes & QC2 (KODEL)

- New
- Reinforced
- Modified

1. Washing Bakelite surface with MEK and selection
2. Graphite printing, inspecton, and measurement of surf. Resistivity (QC2)
3. Visual inspection for HPL panels (QC2)
4. PET coating (insulation) and inspections (QC2)
5. Gluing electrodes
6. Gas Leak & spacer bonding test (QC2)
7. Linseed oil varnishing and inspection (QC2)

9. EVA-glue sealing along the peripheries of electrodes
10. Cabling (HV and ground)
11. 3-step HV test (QC2, std. TFE-based gas mixture)
12. Final visual inspection (QC2)
13. Packing & shipping to assembly sites

Outsourcing to private companies

Brushing and washing with MEK for HPL

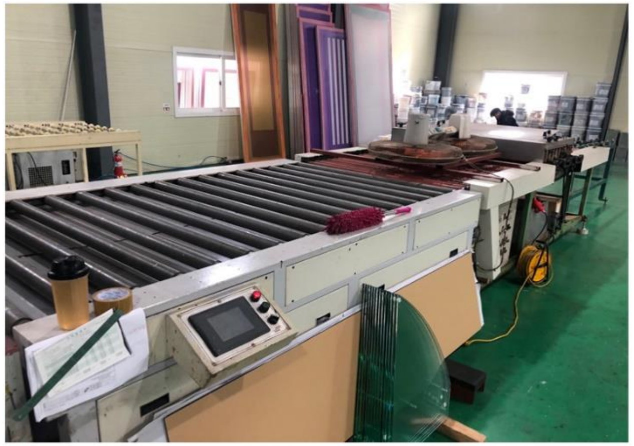

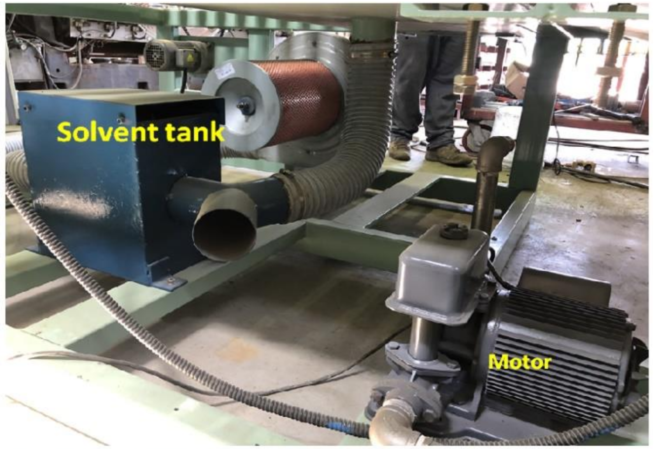

Brushing scheme
- ✓ Two PE brushes (top)
- ✓ Two metal brushes (bottom)

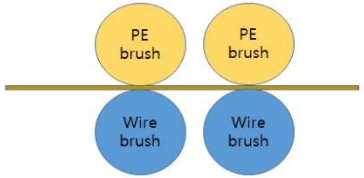

Graphite printing facility

More uniform surface resistivity ranging from 300 to 700 kΩ/sq

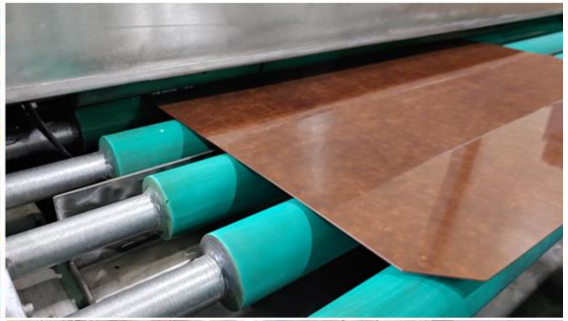

Outsourcing to private companies

PET-film coating procedure (new)

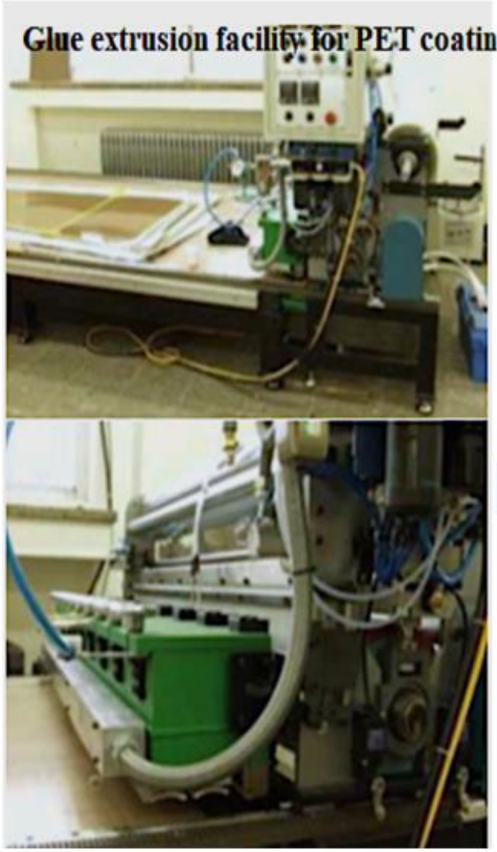

NEW

Vacuum gluing facility @Yurim

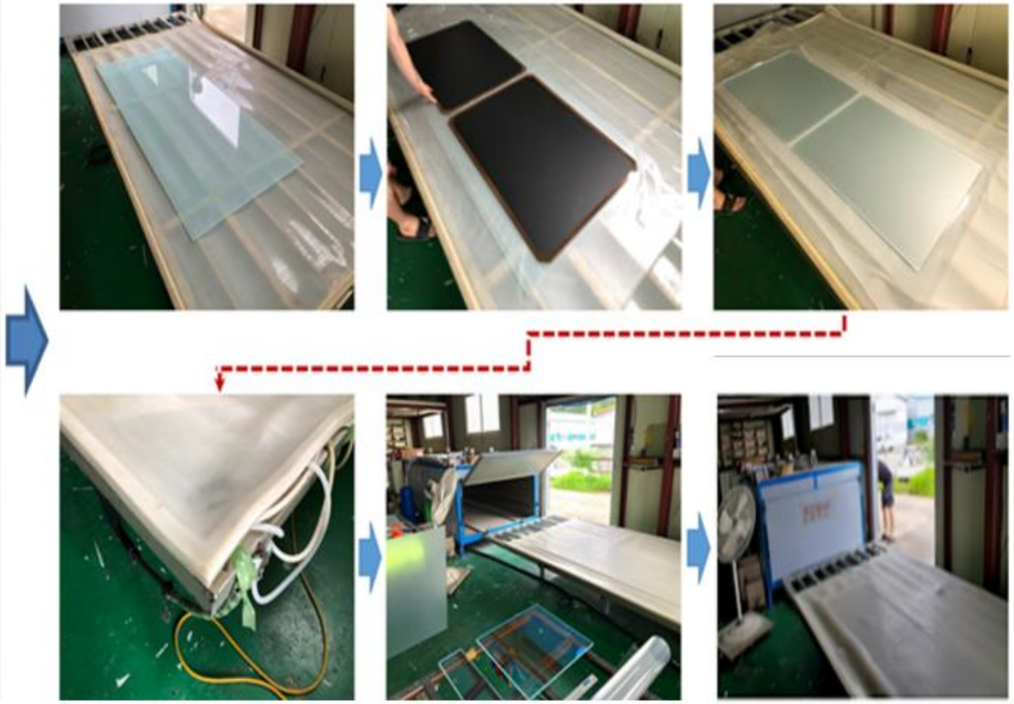

Steps

1) Place 250-μm thick EVA glue film on HPL

2) Place 190-μm thick PET film on the EVA-film covered HPL

3) Insert ~ 5 layers in a vacuum chamber

4) Increase the temperature to 90°C for 60 mins.

5) Cure adhesiveness of the glue on PET @90 °C for 60 mins

6) Gradual decrease of vacuum temperature for 60 mins

At KODEL

Minho Kang at KPS meeting on April 2020

Gluing RPC electrodes (gas gaps)

Gas Nozzle

Gluing tables and pressure devices

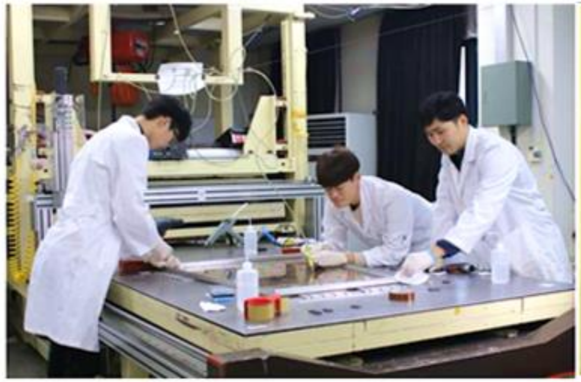

Metric tables and multi-layer air pouches for gluing and glue hardening for gaps

Air pouches uniformly press the whole surface of the gap with a pressure of 30 hPa (equivalent to 300 kg m^{-2}).

Spacer jig

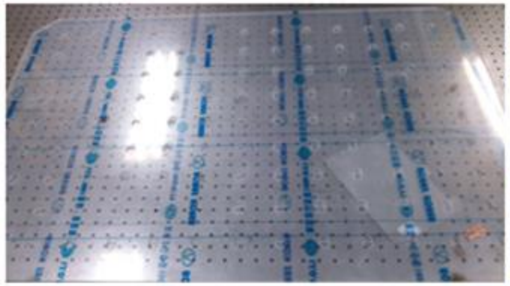

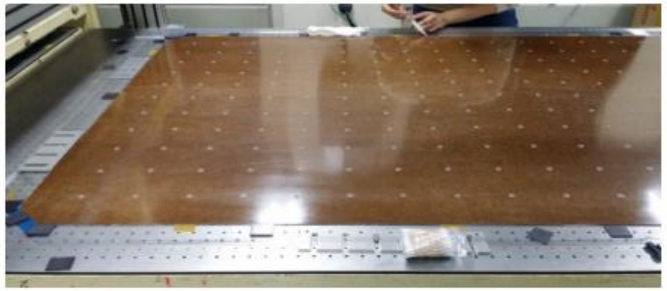

Gap supporting m

peripheral strip spacers

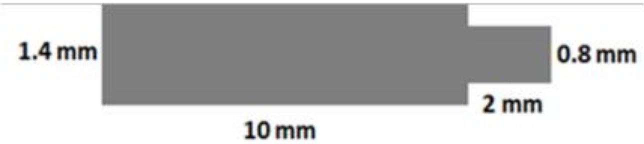

gas-inlet profiles

circular spacers

Epoxy glue (3M DM460):
hardening time ~ 24 h
Requiring epoxy out gassing for additional 48 hours before oil varnishing

At KODEL

Linseed-oil vanishing and drying

Procedure of the linseed-oil varnishing using a facility composed of compressors, an oil tank, and a lifting device.

Oil mixture: 50% linseed oil + 50% heptane

Speed of the lifting device = 0.3 mm/s

Quick double oiling @T=28 °C

Apply drying gaps with compressed air

@T=30 °C for 120 h and

@ room temperature for 24 h

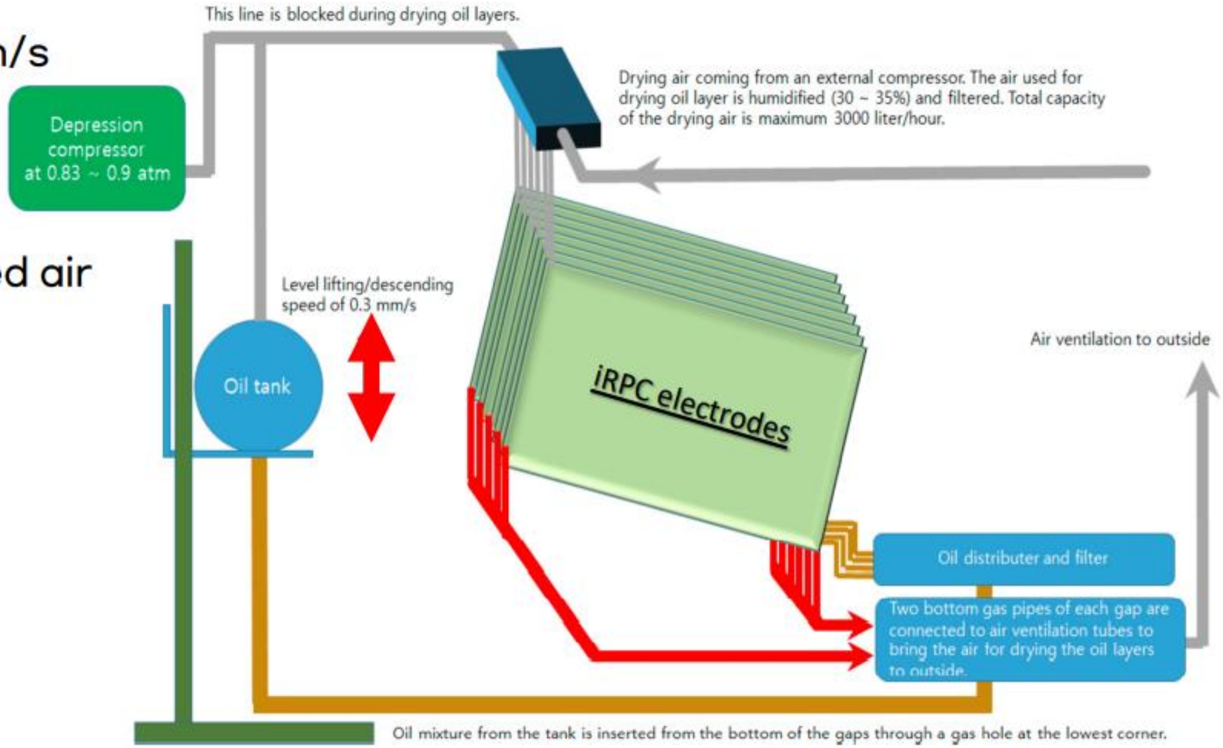

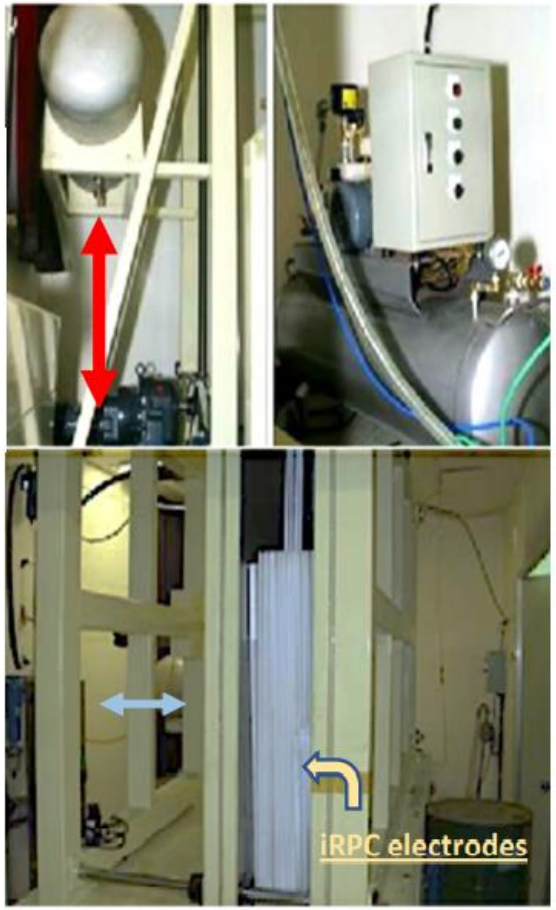

At KODEL

QC2 step1: gas leak & spacer bonding

Requirements:

For gas leak, pressure drop of a successful gap @+15 hPa should be less than 0.4 hPa for 10 mins.

Spacer bonding: no single spacer failure allowed.

- QC data : cvs excel format for pressure tests

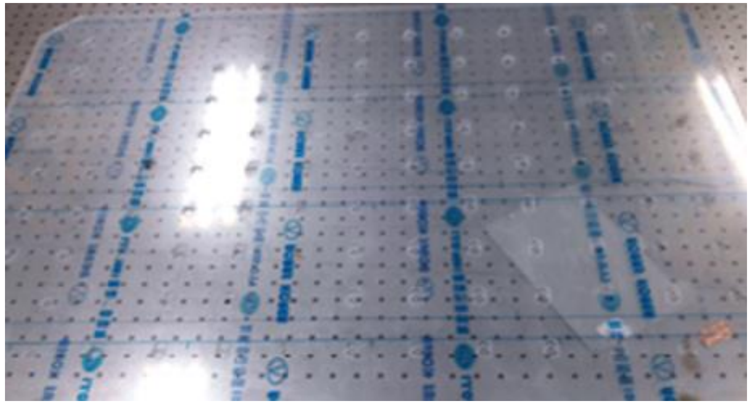

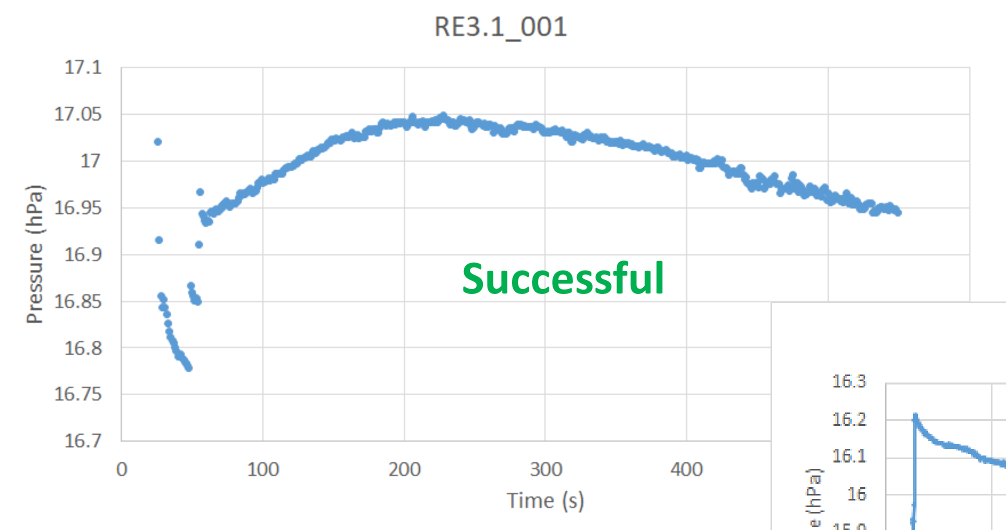

For 1st RE3.1 batch (18 gaps), 1 gap with a spacer failure

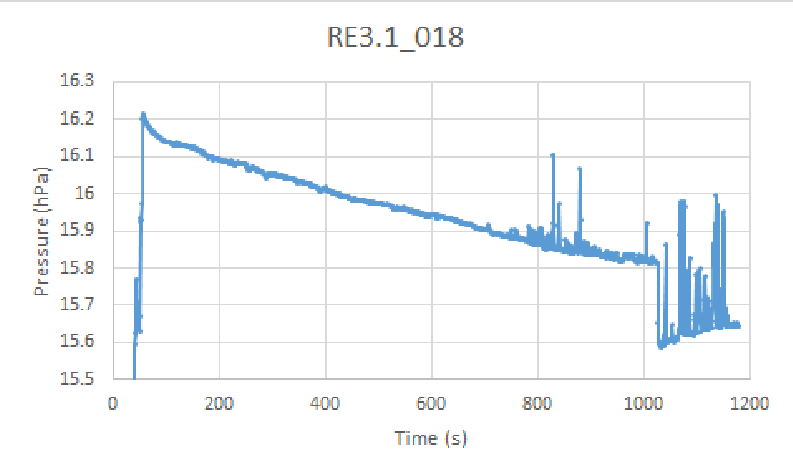

RE31_gap_number_tmp	delta P (hPa)	# of failed spacer
3C38E220427311602	0.16	0
3C38E220427321602	0.34	0
3E38E220427311604	0.20	0
3E38E220427331604	0.00	0
4A38E220427311605	0.16	0
4B38E220427311606	0.00	0
4B38E220427321606	0.20	0
4B38E220427331606	0.21	0
4C38E220427311607	0.16	0
4C38E220427321607	0.06	0
4C38E220427331607	0.20	0
4D38E220427311608	0.36	0
4D38E220427321608	0.19	0
4D38E220427331608	0.15	0
4E38E220427331609	0.10	0
4E38E220427331609	0.30	0
5B38E220427311611	0.00	0

At KODEL

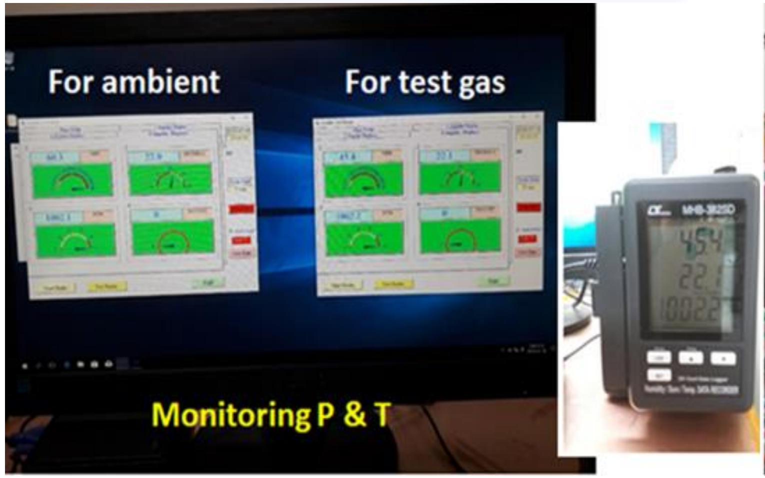

QC2 step2: three-step HV tests

1) 1st HV scan test
2) Long-term test for 120 hours
3) 2nd HV scan test

Operational gas = 95.2% TFE + 4.5% isobutene + 0.3 SF_6 with Gas humidity = 40%

Requirements:

For Ohmic current: current limit = 0.5 µA @5.0 kV

For operation: current limit = 2 µA at effective HV (7.5 kV)

- QC data for HV tests: csv excel format for currents, P, T, H (gas & ambient)

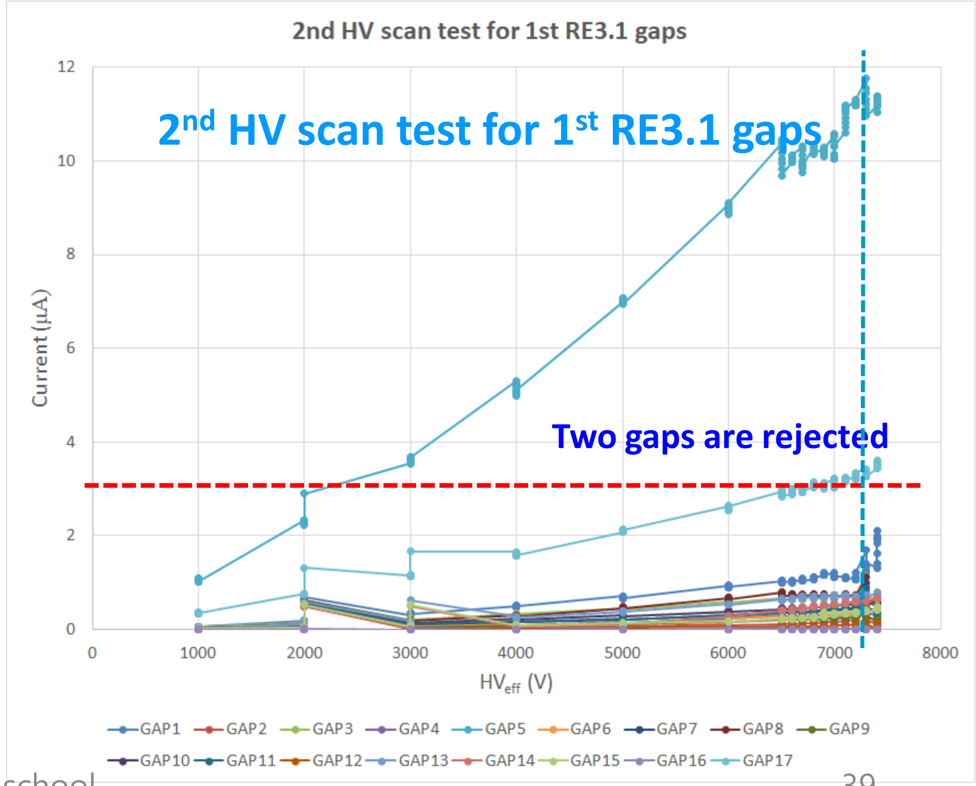

MPI: qualification of 2 industrial producers Francesco and Oliver

MIRION TECHNOLOGIES

Website:
https://www.mirion.com/

PTS Maschinenbau

Website:
https://www.ptsmaschinenbau.com/

The 2 producers are followed up directly by MPI personnel and based on the same design and equivalent procedure been implemented by INFN at GTE

- ✓ PHASE-0: Optimization of the production steps in interaction with companies
- ✓ PHASE-1: Qualification of companies with test-sample prototypes
- PHASE-2: Qualification of companies with both small- and real-scale prototypes ← **we are HERE!**
- The series production is planned to start for September 2024

Certification plan

- Small- and real-scale RPCs will undergo long-term irradiation for half a year in the CERN GIF++
- Small and real scale prototypes per each company + dummies for oiling QC
- Small scale RPC are produced and just started irradiation at GIF++
- Real scale prototypes are under construction

Factory Acceptance Tests

An extensive Quality Assurance and Quality Control (QA/QC) program has been established to guarantee high quality and reliability of the gas volume production:

QA/QC step 1: HPL production test

- ➢ Visual inspection of surface, volume resistivity meas., thickness meas.

QA/QC step 2: Electrode production test

- ➢ Visual inspection and surface resistivity meas. of the graphite coating.
- ➢ Test of absence of bubbles between the insulating PET foil and the graphite coating.

QA/QC step 3: Gas gap production test

- ➢ *... see next slides!*

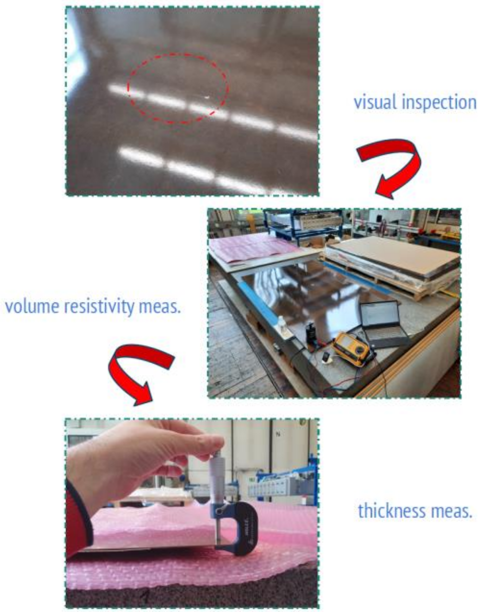

Spacer traction test & Spacer height measurement

Objective:
Ensure the reliability of glued pillars on HPL plates for assembled gas volume.

Methodology:

- ➢ For each gas volume, a 3×3 cm² HPL-spacer-HPL sandwich sample is prepared at the end of each gluing phases.
- ➢ A traction force of 30 N is applied to each sample to ensure that no disconnection occurs.
- ➢ If no disconnection occurs at 30 N, the applied force is gradually increased until the pillar breaks.

Analysis:
The breaking point occurs at a traction force ≥ 100 N.

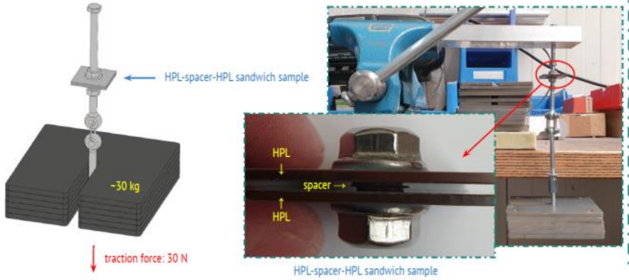

Objective:
Ensure precise compliance with spacer height during the gas gap gluing phase, serving as an indirect verification of accurate gas gap dimensions.

Methodology:
Following the initial gluing step, the spacers remain accessible, allowing for precise measurement of their heights relative to the HPL plate using a digital drop indicator.

Analysis:
All spacer heights are within the 1 mm gas gap specification, with a spread well below 20 μm.

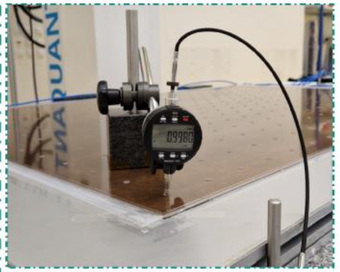

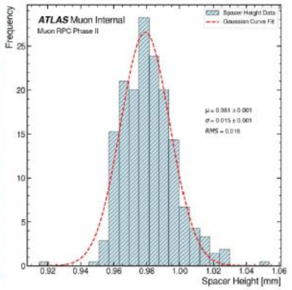

Gas tightness measurement

Objective:
Identify the gas leak rate of the gas gap by monitoring the drop of the internal over-pressure as a function of time and check the gas tightness

Methodology:

- ➢ The internal pressure of the gas volume is increased by up to 3 mbar above atmospheric pressure using a controlled gas supply.
- ➢ The internal pressure is monitored for 15 min. after closing the gas volume.

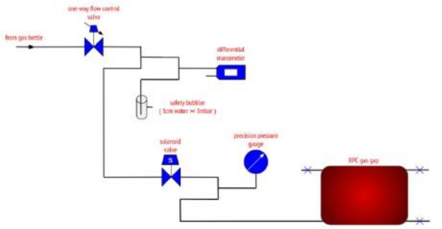

Analysis:

- ➢ The experimental data are modeled using both linear and exponential fits to determine the gas leak rate of the gas volume
- ➢ The gas volume passes the gas tightness test if the gas leak rate of the gas gap + gas system does not exceed: - 9.7 × 10^{-4} mbar × l / s.

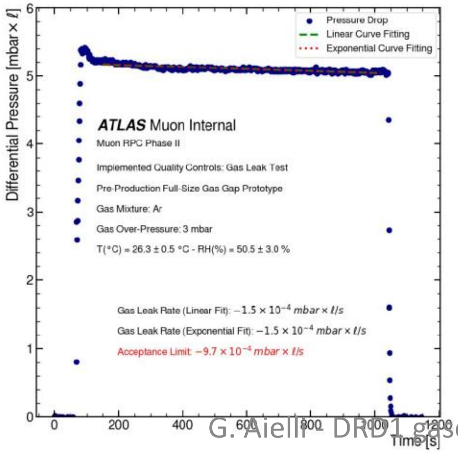

Leakage current measurement

Objective:
Measure the leakage current within the HPL electrodes of the gas volume to ensure proper insulation and minimal leakage.

Methodology:

- ➢ The HPL electrodes are subjected to the same voltage as the HV power supply.
- ➢ A copper-coated aluminum bar, grounded through a 100 kΩ resistor, is brought into contact with the long side of the gas gap under test.
- ➢ The leakage current flow to ground is measured using a digital multimeter, by monitoring the voltage drop across the resistor.

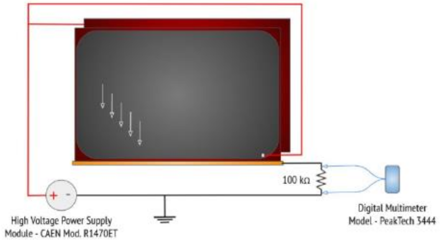

Analysis:
The gas volume passes the leakage current test if the leakage current not exceed 200nA at the maximum applied voltage of 8 kV on both HPL electrode.

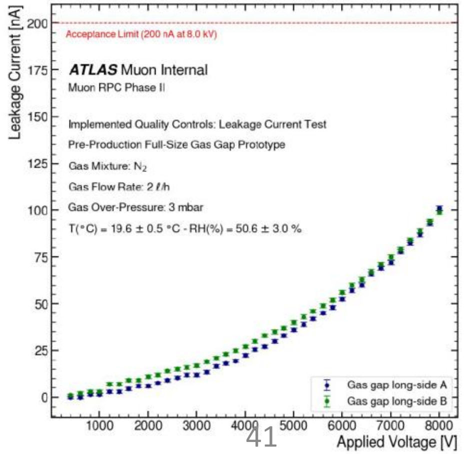

The platform of gas gap production at USTC

- A marble table as base:

  2.5m×1.8m

- A head stock supported by a gantry moving in 2-dimentional
- 9 holes among the table are connected to the vacuum system.

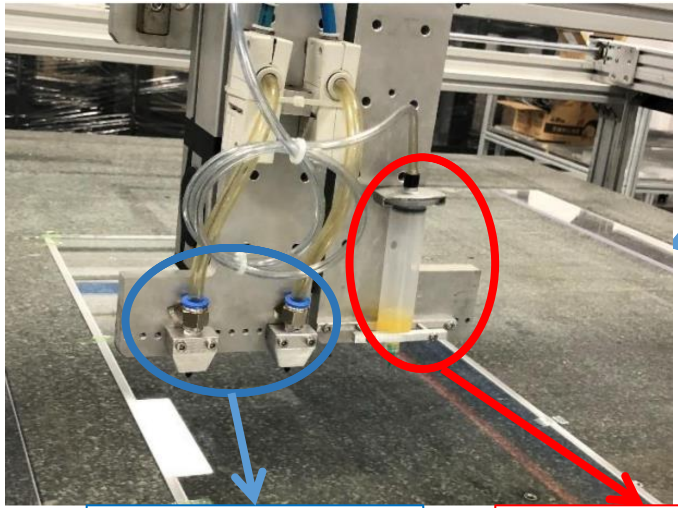

Spacer pickers

Glue syringe

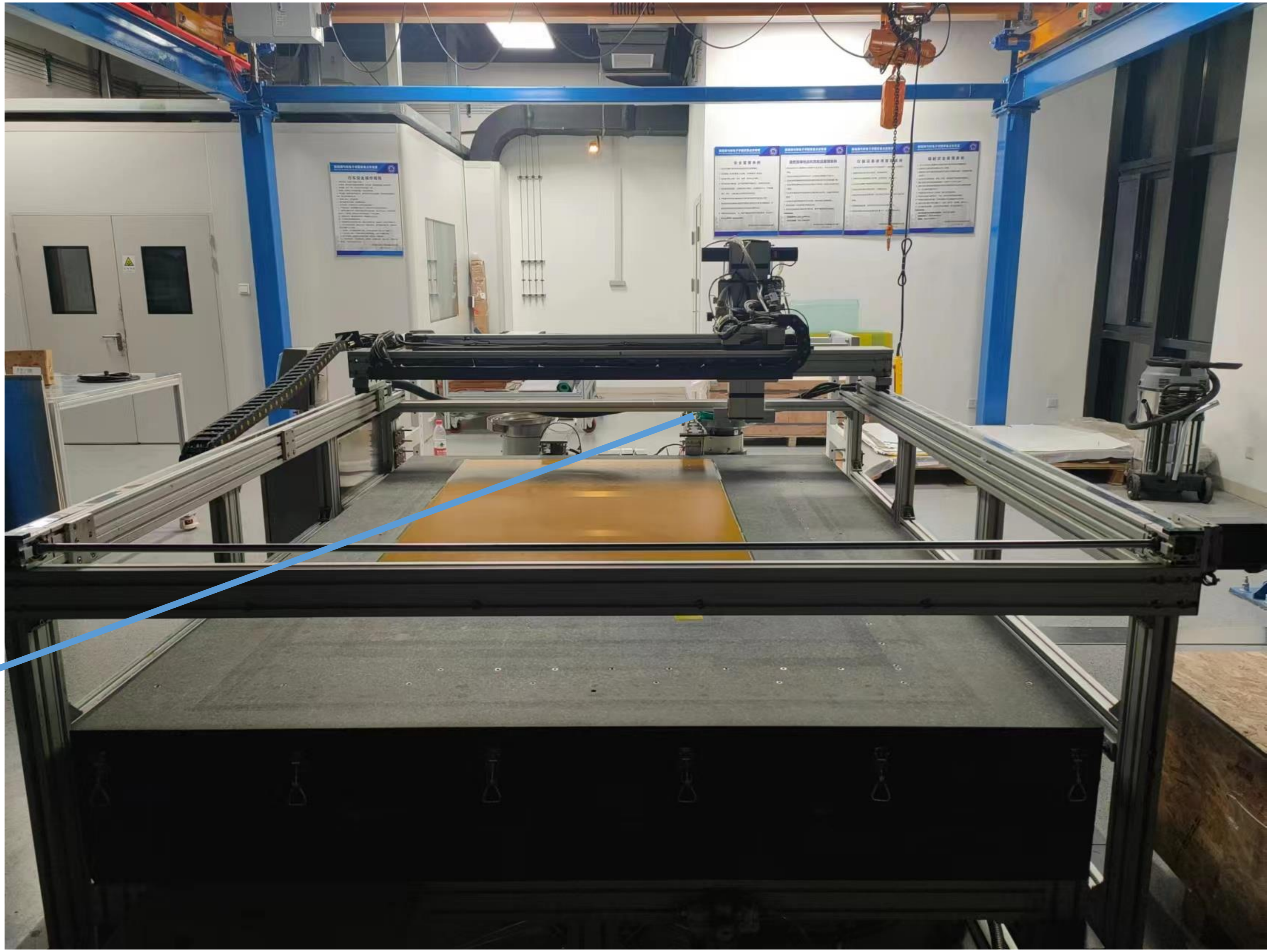

Production steps

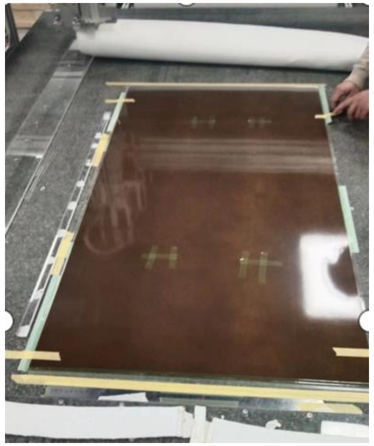
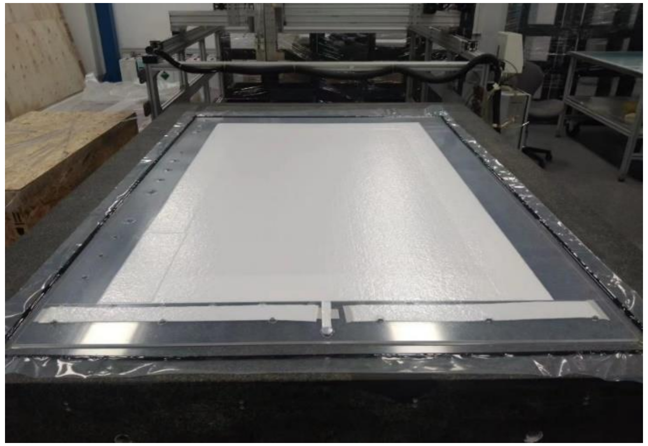
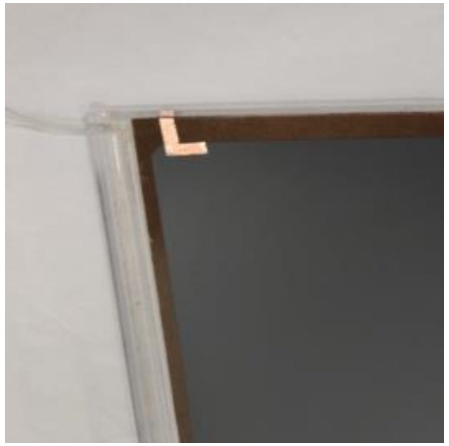

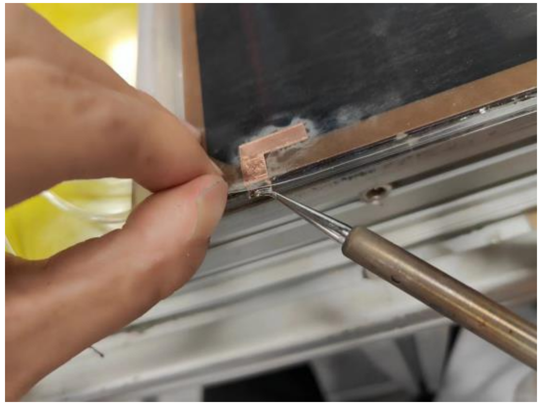

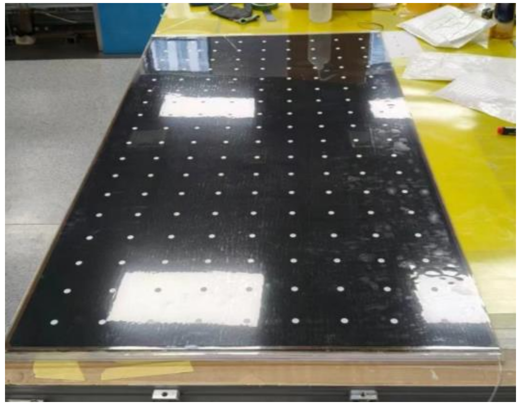


Backup

Space resolution principles

- Space resolution is driven by 2 factors
  - Intrinsic localization of the event
  - Precision of the chamber geometry

MPGD

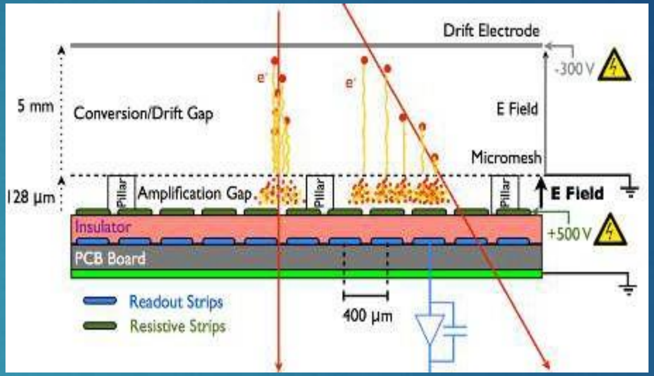

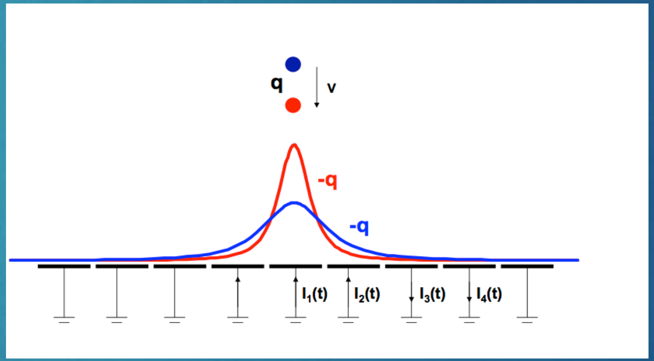

RPCs

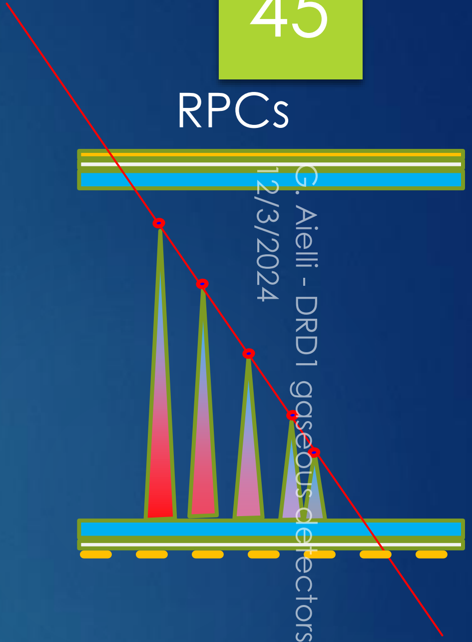

Wire chamber

$$E \approx \frac{1}{r}$$

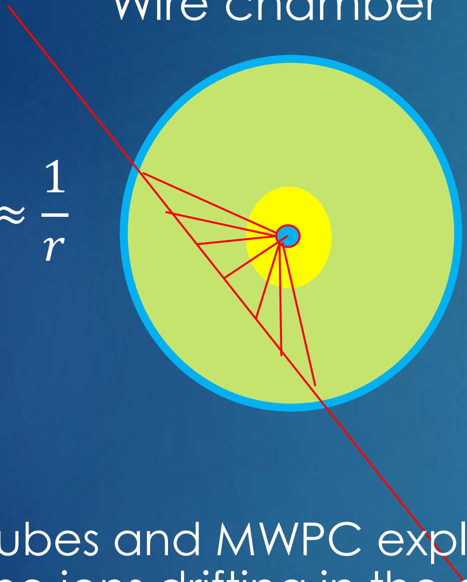

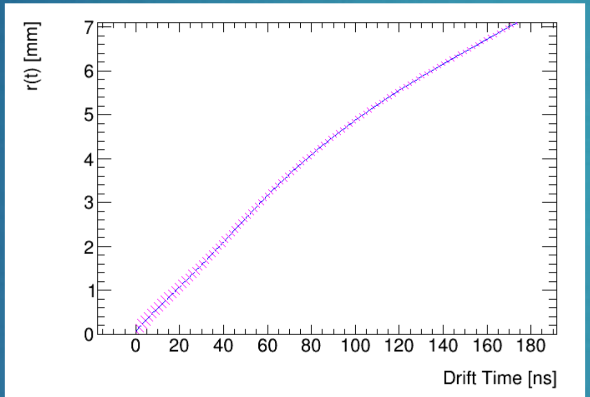

- Tubes and MWPC exploit the R-t relation of the ions drifting in the gas and rely on their metallic bulks which can be easily machined to offer a precise reference frame. Can obtain high precision with low channel density

- RPCs and MPGD exploit electrostatic induction of the moving charges to calculate the charge centroid. The resolution is driven by the readout system segmentation and mechanical precision preserving it on large multi-layer chambers made of composite materials. Can obtain high precision with high channel density

The Physical model

An induced charge distribution model

The main limitation of this model is that it does not take into account the presence of the resistive electrodes. It also neglects the presence of other parameters, as graphite painting.

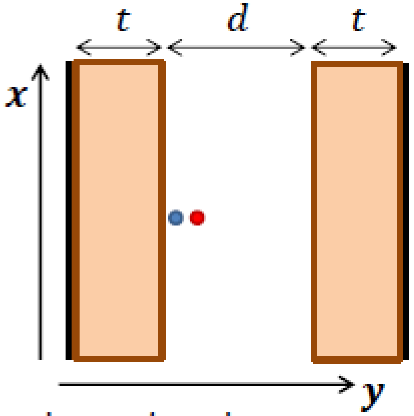

Considering the presence of the electrodes, the parameter δ can be written as

$$\boldsymbol{\delta \cong \frac{d+2t}{\pi}}\ ^{*}$$

*C. Lu, Princeton University, Princeton, NJ 08544, USA SNIC Symposium, Stanford, California – 3-6 April 2006

For simplicity, when the thickness of the electrode is similar to the gas gap and smaller than the strip pitch, the effect of the charge displacement with respect to the middle of the gap is negligible. This offers the possibility to use the model.

$$\sigma = \frac{q_{ind}}{2\pi\delta} \frac{1}{cosh\left(\frac{x-x_0}{\delta}\right)} \quad , \quad \delta \cong \frac{d+2t}{\pi} \quad , \quad q_{ind} = q \frac{\Delta y_{el}}{d + \frac{2 \cdot t}{\varepsilon_r}}$$

L. Paolozzi, RPC2014 - Beijing 4

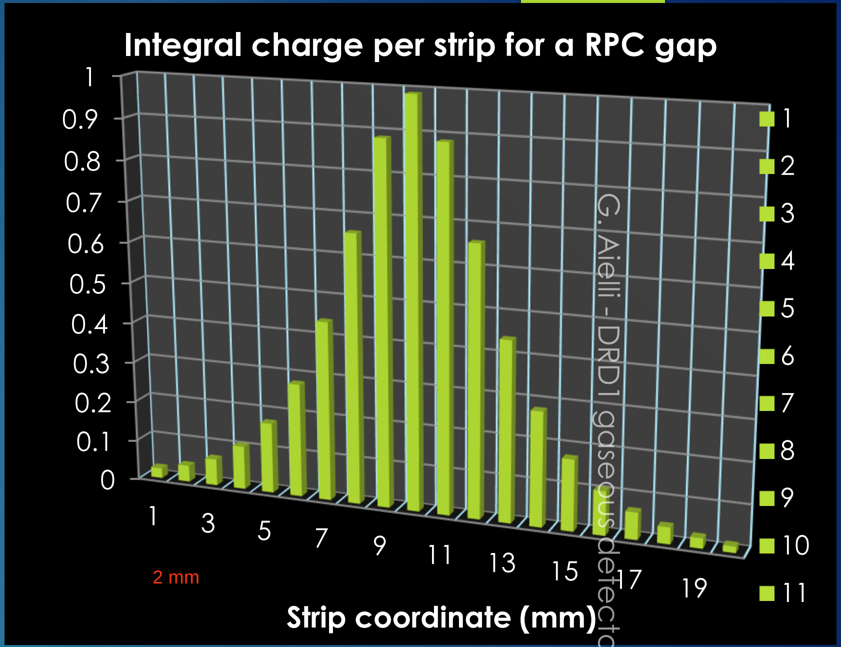

$$\sigma(x,\bar{x}) = \frac{A}{\cosh\left[(x-\bar{x})/\delta\right]}$$

$\Rightarrow$ integratin g over each strip

$$Q_i = \int_{x1}^{x2} \frac{A}{\cosh\left[(x-\bar{x})/\delta\right]} = $$

$$= A\delta \cdot arctg\left[\left(e^{(x-\bar{x})/\delta}\right)\right]_{x1}^{x2}$$

Yet another method: strip drift time

Challenging readout for future colliders

- Fast leading signals for thin gas gaps
- New generation of inexpensive ~ 1ps TDCs
- Propagation speed 15 cm/ns
- 100 μm precision is the target
- Can be replicated in 2D
- Accurate reconstruction of multiple tracks

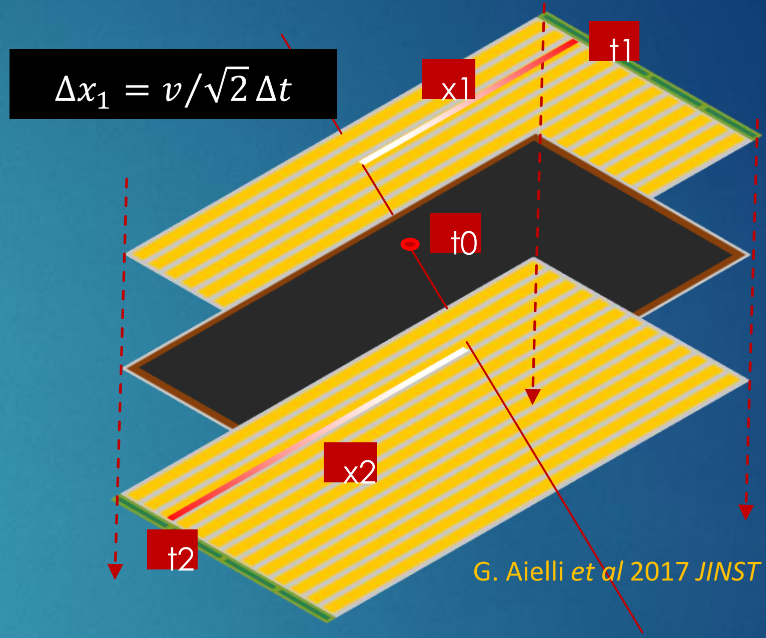

G. Aielli *et al* 2017 *JINST* **12** C01057

A new method: the planar drift chamber

- Planar detectors can generate signals with accurate position information → discharge cell footprint ~ 100μm^2 (10.1088/1748-0221/7/11/P11012)
- Same limitations of micro-pattern detectors coming from
  - the readout system precision
  - Expensive readout electronics
  - A lot of readout channels
- Efficient and innovative readout systems
- Applications: PET, muon tomography, future tracking devices

10.1088/1748-0221/11/11/C11008

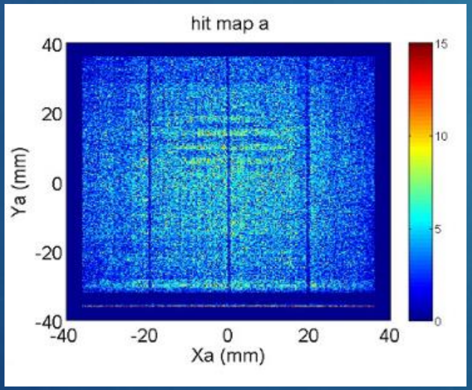

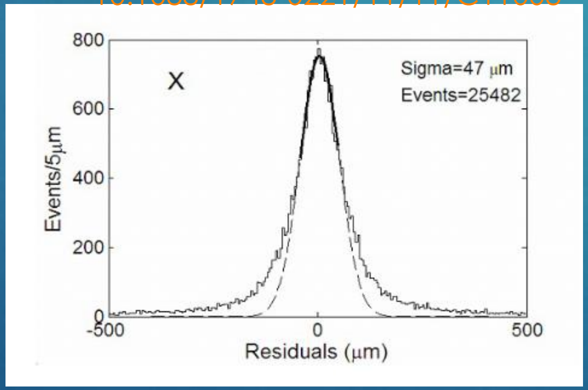

A NEW IDEA → PLANAR DRIFT CHAMBER

- MEASURING THE IMPACT POSITION FROM THE DIFFUSION WAVE TIME WALK DIFFERENCE ON THE GRAPHITE ELECTRODE

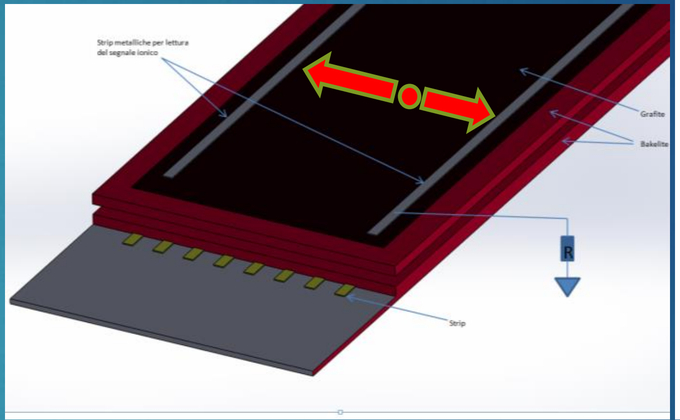

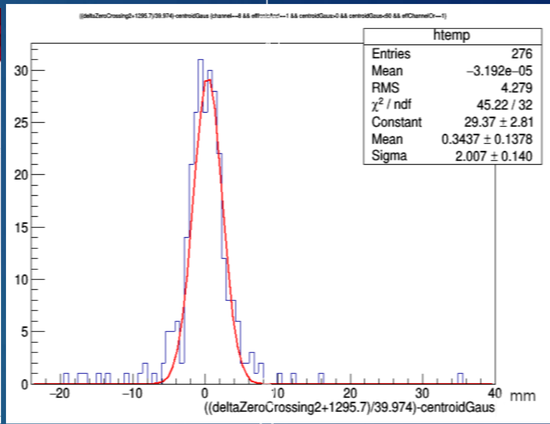

R. Cardarelli et Al. Track resolution in the RPC chamber NIM A572, vol. 1 170-172 (2007).

- CAN REACH SUB MM PRECISION
- SUITABLE FOR LARGE AREA LOW RATE ENVIRONMENT (RATE IS LIMITED TO ABOUT 100 HZ/CM^2)
- VERY LOW COST READOUT ELECTRONICS

Space resolution performance

RPCs and MPGDs

- ATLAS MMGAS
  - resolution ~ 100µm with 0.4 mm strips
- The drift gap is large → impact angle worsen resolution corrections needed (micro-TCP method)
- Affected by the B field
- A lot of care needed in construction
- Proof of principle on a small MRPC
  - resolution ~ 50µm with 4 mm strips
  - RPC less sensitive to the angle → smaller gas gaps and a single dominant cluster
- 1m2 1mm gas gap ATLAS prototype reaching 1mm space resolution with 2.7cm strip pitch! Up to 10 kHz/cm^2 at GIF++
- Space resolution is not a classic RPCs performance, though physics is not preventing it…

MMGAS

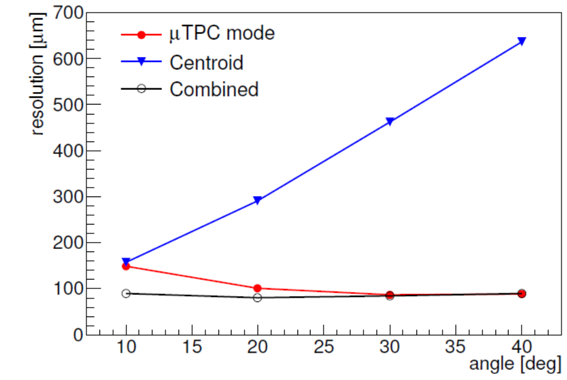

MRPC

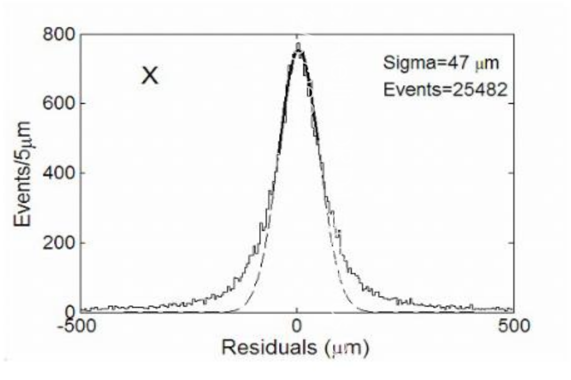

Planar technologies need further R&D for a simple and reliable structures to emulate DTs

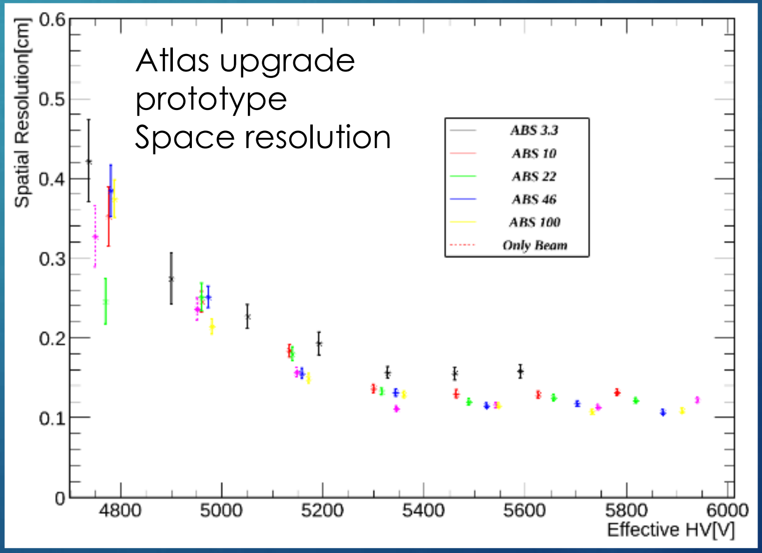

Space resolution performance

Drift tubes (ATLAS case – CMS is similar)

- Examples: ATLAS and CMS DT systems
- Great improvement by reducing the drift length
- Wire accuracy 20μm, resolution < 80μm
- Angular resolution independent on the track angle
- Self calibrating
- Angular resolution < 70 mrad with 2x4 tube layers
- Mechanically stable over large areas

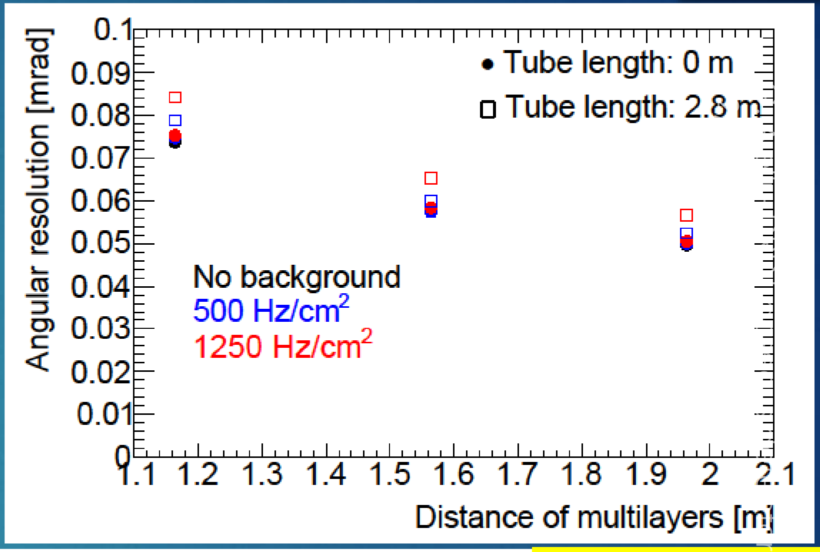

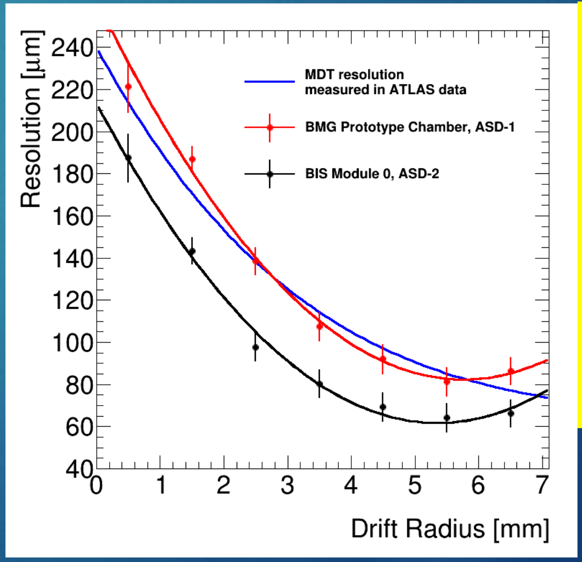

Drift tubes are at the moment a more reliable and simpler tracking technology with respect to planar detectors

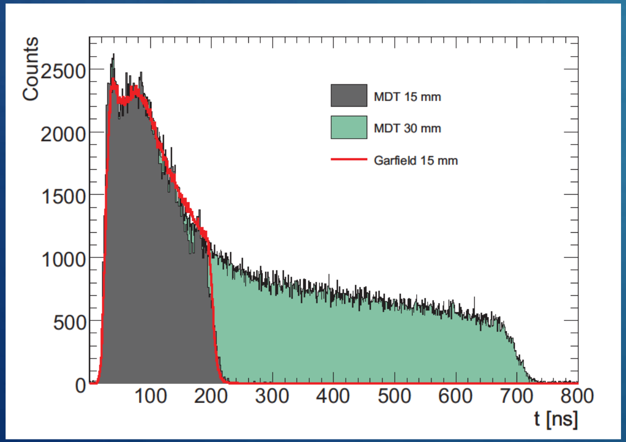

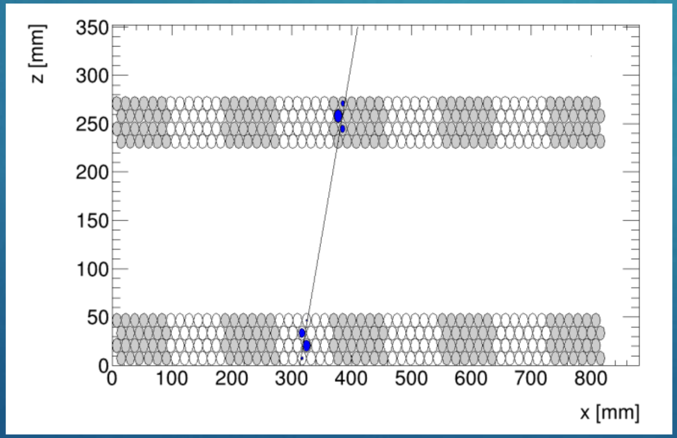

Time resolution principles

- Time resolution is driven by
  - Avalanche statistical fluctuations
  - Drift time (velocity x gap size)
  - Electronics noise

Wire chamber

$$E \approx \frac{1}{r}$$

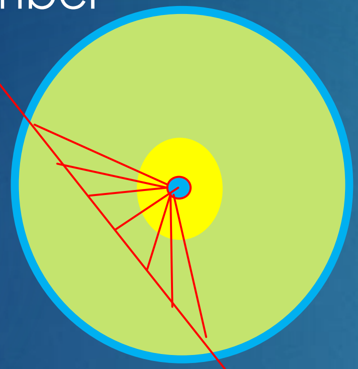

MPGD

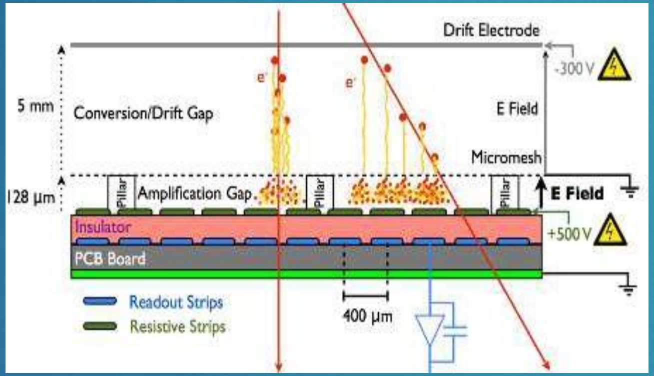

$$E \approx \frac{1}{r}$$

- MWPC and MPGD work on similar principles: the separation of the drift and multiplication introduces irreducible uncertainty on the time resolution, dependent on the drift width

- RPCs and MRPCs drift and multiplication space coincide. The multi-micro gap RPC segments the gas gap to further reduce the drift time

RPC time resolution

Time resolution is one of the main RPC features

- Golden standards: **MRPCs ~50 ps** -- **RPCs ~500 ps**
- complex physics behind: cluster statistics, multiplication dynamics, electronic noise
- Empirically smaller gas gaps → higher resolution
  - Smaller gas gaps can be operated at higher electric field and have a faster multiplication dynamics compressing noise fluctuations
- As one learn from other detectors the electronics noise plays a role

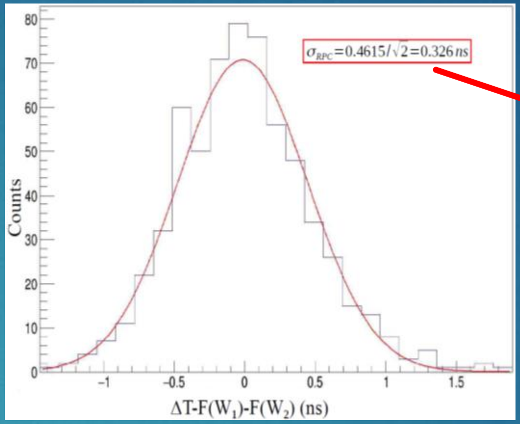

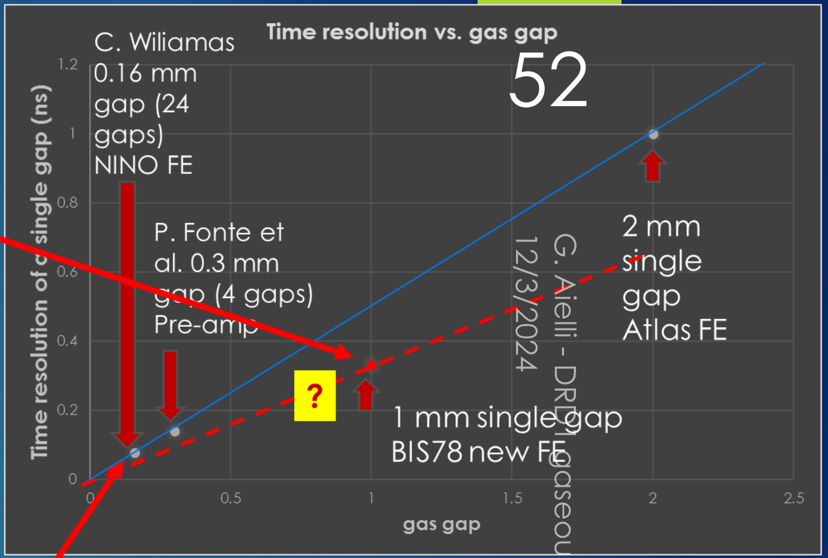

- ATLAS UPGRADE **5 PC** → 4 fC FE TH. → 4×10^3 E-
- ATLAS UPGRADE **6 PC** → 40 fC FE TH. → 4×10^4 E-
- ATLAS AND CMS **30 PC** 50 fC FE TH. → 5×10^4 E-

CHALLENGE: RESOLUTION BEYOND 50 PS

- WITH MORE AND THINNER GAS GAPS, E.G, 20 PS WITH 24, 0.16 MM GAPS [10.1016/J.NIMA.2008.06.013]
- THINNER ELECTRODES → HIGHER SIGNAL
- LOW NOISE HIGH RESOLUTION FEE (PICOTDC) HTTPS://KT.CERN/TECHNOLOGIES/PICOTDC

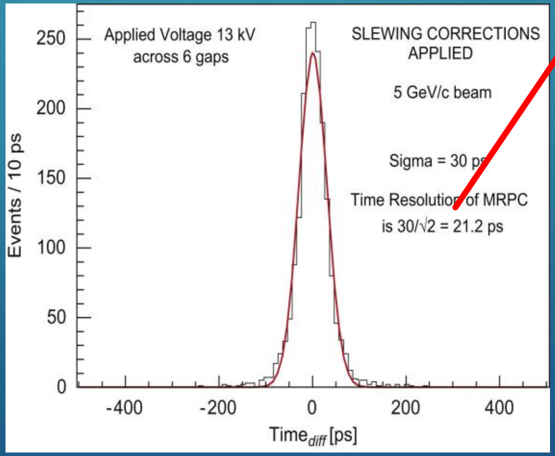

INNOVATIVE APPROACH →

- GOING BEYOND THE GAS GAP WIDTH LAW
- EXTRACT HIDDEN INFORMATION BEYOND DISCR. AND SLEW CORRECTION
- PROMISING THE USE OF DNN TO FILTER THE COMPLEX AVALANCHE DYNAMICS → 16 PS ACHIEVED! [ARXIV:2005.03903V1 [PHYSICS.INS-DET] 8 MAY 2020]

Drift based detectors time resolution

- DT drift spectrum is by construction unsuitable for timing as a long drift time is used for high space accuracy
- ATLAS Thin gap chambers → 6-7 ns
- Typical Micromegas, GEM, μRWELL 10 ns
- A proposal to get rid of the drift variations is to hybridize a MMGAS with a photo-cathode and a Cherenkov radiator. Resolution ~ 50 ps driven just by the single avalanche process, like in MRPC

Atlas MMGAS

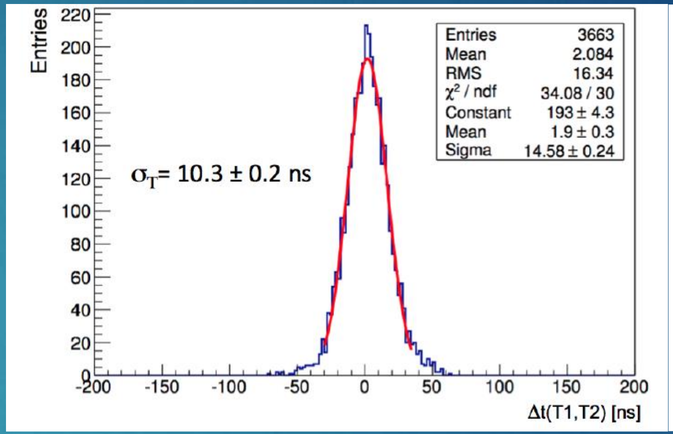

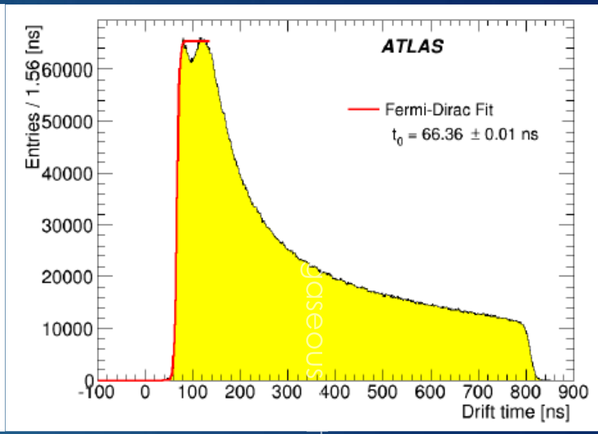

Atlas sMDT

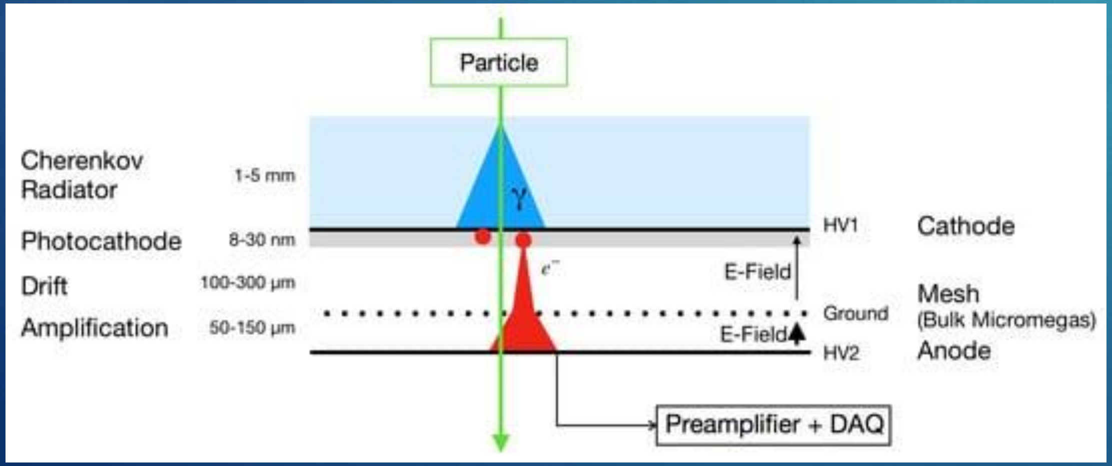

- Drift detectors and limited in time resolution and an optimal strategy is combining a drift detector with an RPC to have a combined performance.
- MPGD have a barely sufficient resolution for identifying the BC at 25 ns but it can be improved by using multiple layers for the 5ns scenario
- The idea to combine a Cherenkov and a MMGAS can provide a good timing in the very high rate regions (why not an RPC?)

Present limits – rate and longevity

Rate capability [RPCs and MPGDs]

- Electrode resistivity to prevent discharges in RPCs and MPGDs but limits rate capability:
  - ΔV = <**Q**> x freq. x **R**
- <**Q**> is very favorable in MPGDs

Longevity: Bulk materials insensitive to radiation, but

- radicals produced in RPC avalanches affect the electrodes
- High ionization may induce discharges in MPGDs progressively damaging the detector

Rate capability(drift chambers)

- Limited by the space-charge effect
- Effect reduced with R^3 → R=1/2 → rate = 8x (drift time x cross section)

Longevity: Bulk materials insensitive to radiation, but

- Gas purity is very important to avoid ageing
- no discharges possible (geometrical quenching)
- No observed ageing in such conditions

- Lowering R improves rate capability only
  - Lower resistivity materials
  - Thinner electrodes
- Achieving high rate by brute force reduction of R (without reducing at the same time the E field) may lead to instable detectors

- Reduction of <Q> improves rate capability and longevity at the same time
  - by improving the S/N on the FE electronics
  - by improving the signal collection efficiency

Keeping the gas clean is the key to preserve the electrode longevity

High rate for single gap RPCs

- limited by Ramo theorem (~1/20 of <Q> is usable)
- low resistivity electrodes made of HPL (~10^{10} Ω cm)
- SiGe FE tech. with 4k e- noise to reduce <Q>
- Reaching up to 10 kHz/cm^2 in production chambers
- Suitable for safe operation with eco-gas mixture

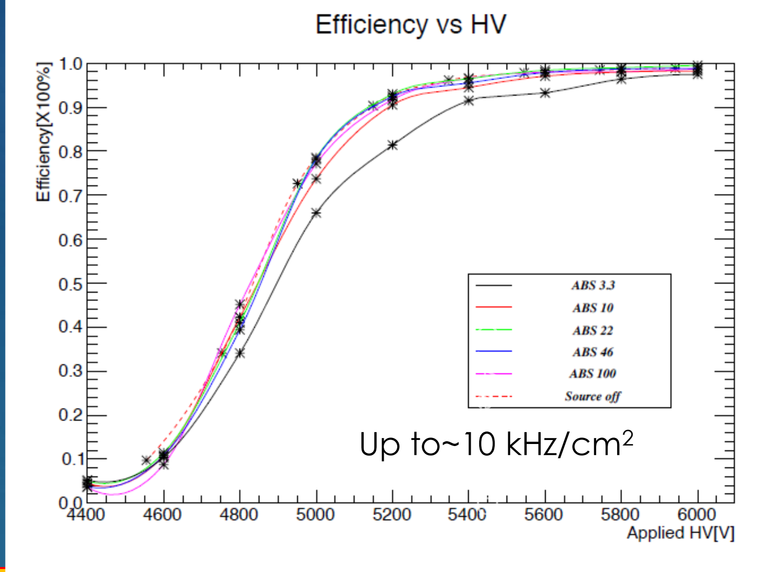

FFC full TARGET → improve by a further order of magnitude by increasing S/N and lowering R:

Last generation SiGe etero-junction technologies (fT 0.7 THz) announce a further x 10 leap in the FE → 500 e- noise reduction

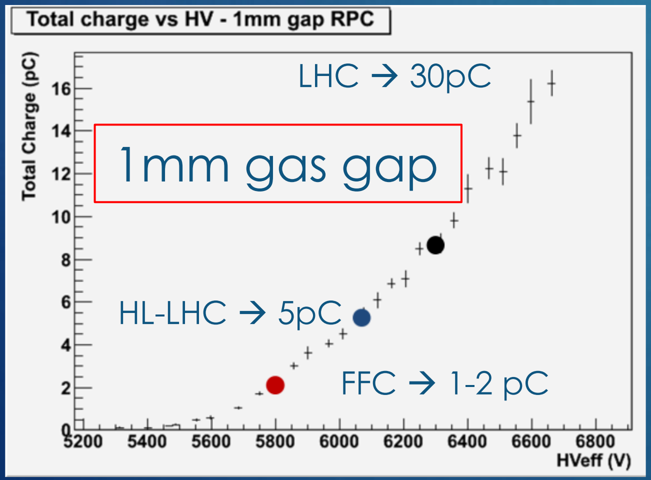

For further exploiting the electronics:

- Faster avalanche
- Very efficient grounding

A new device: single gap semi-conductor RPC

[electronic carriers can not be depleted]

- 0.6 mm GaAs electrodes
- Resistivity 1.4×10^8 Ωcm
- Tested up to > 40 kHz/cm^2
- > 1 MHz/cm^2 is possible
- Active area 6.25 cm^2
- 10.1088/1748-0221/15/12/C12004

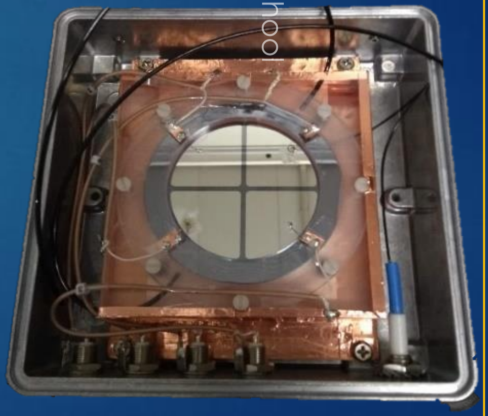

The logistic saturated avalanche model

Logistic Avalanche

- Townsend, Rather, Meek et. al developed a complete description of the avalanche growth under the approximation of independent electrons
- This is very suitable for describing proportional detectors
- It fails in case of intensive fields growing larger avalanches due to the arising non linear behavior
- The template case is the Resistive Plate Chamber operating with a strong and uniform electric field allowing prompt multiplication of the primary ionization

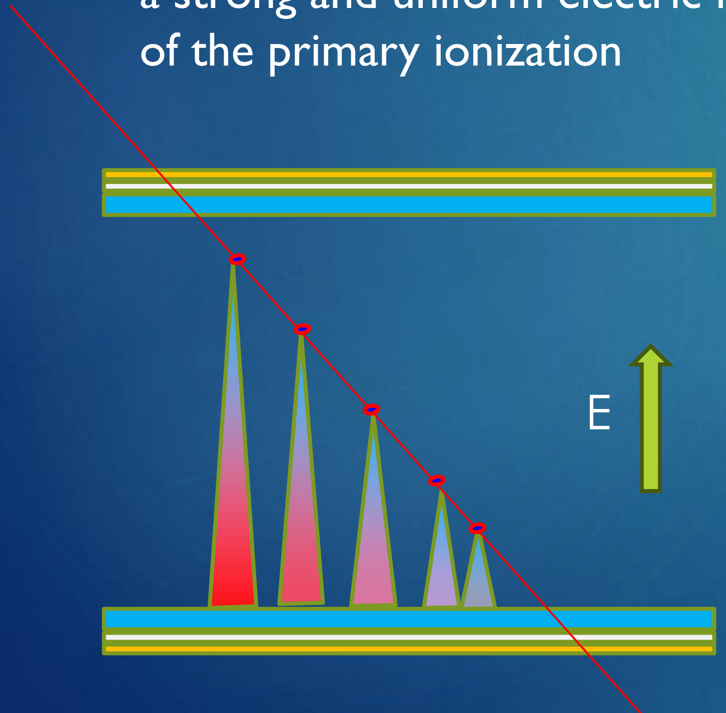

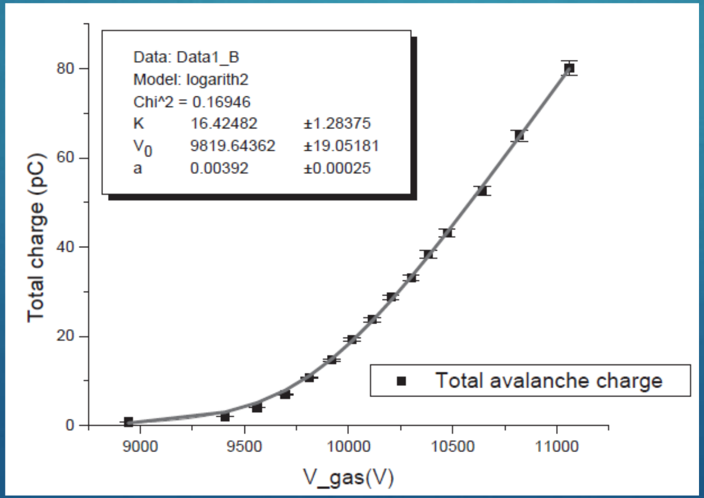

The experimentally observed growth of the avalanche charge recalls the Logistic function introduced firstly in 1845 by Verhulst [8] to describe the growth of a biological population, that tend to become stationary in presence of a limited flow of food resources due to the fact that the number of individuals able to reproduce become constant.

In our case the experimental data on the total charge can be compared with the integral of the logistic function, accounting for the total population: the multiplicating (active) electrons and the spectator electrons

$$Q(V) = K \ln(1 + e^{a(V - V_0)})$$

The logistic avalanche model

- The Logistic equation is obtained by the lowest order non-linear correction to the usual exponential growth equation (equivalent to the Townsend theory

$$\frac{dN}{dx} = \alpha N - \beta N^2$$

$$\frac{dN}{dx} = \alpha N \left(1 - \frac{N}{K}\right)$$

$$K = \frac{\alpha}{\beta}$$

- α and β mean the rate at which the free electrons are created and lost from the active avalanche front.
- The free running variable x in represents system evolution parameters such as the applied field or the avalanche path.
- the growth rate tends to zero as N reaches K
- For β =0 the equations is the classic one

- By integration one obtains the logistic function

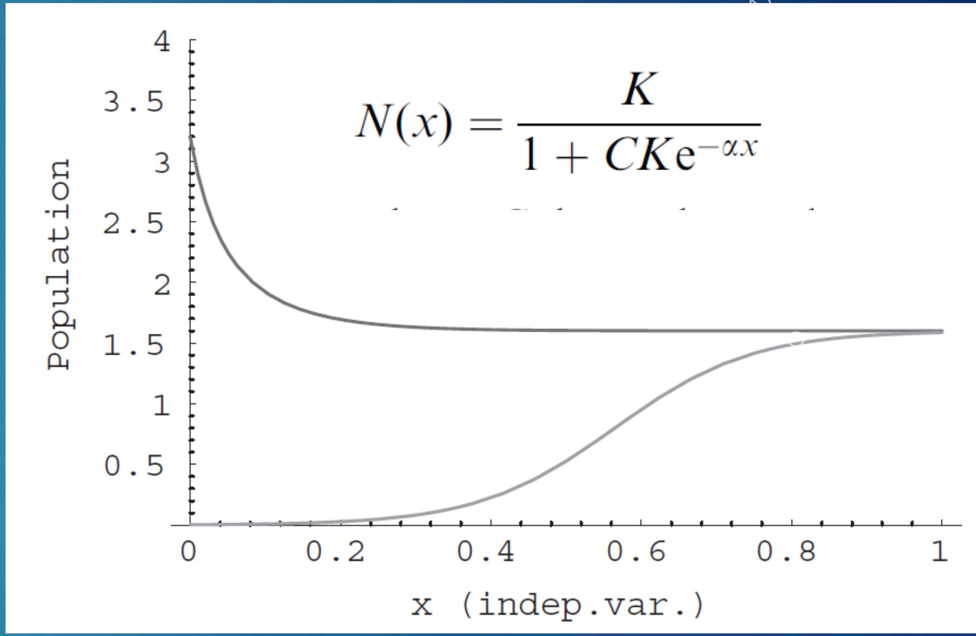

- It describes Qact, the 'active'' avalanche, responsible for the creation of further ionization.
- Qact is a fraction of Qfree

Drift space and V are conjugated

- As a function of the field

$$\frac{\mathrm{d}Q_{\mathrm{act}}}{\mathrm{d}V} = aQ_{\mathrm{act}}\left(1 - \frac{Q_{\mathrm{act}}}{K'}\right)$$

$$Q_{\mathrm{act}}(V) = \frac{K'}{1 + \mathrm{e}^{-a(V - V_0)}}$$

- a is the growth per unit field
- The total collected charge as a function of the applied field is:

$$Q_{\mathrm{tot}}(V) = Q_0 + \int_0^V Q_{\mathrm{act}}(V')a\,\mathrm{d}V' = Q_0 + K' \ln \frac{1 + \mathrm{e}^{a(V - V_0)}}{1 + \mathrm{e}^{-aV_0}}.$$

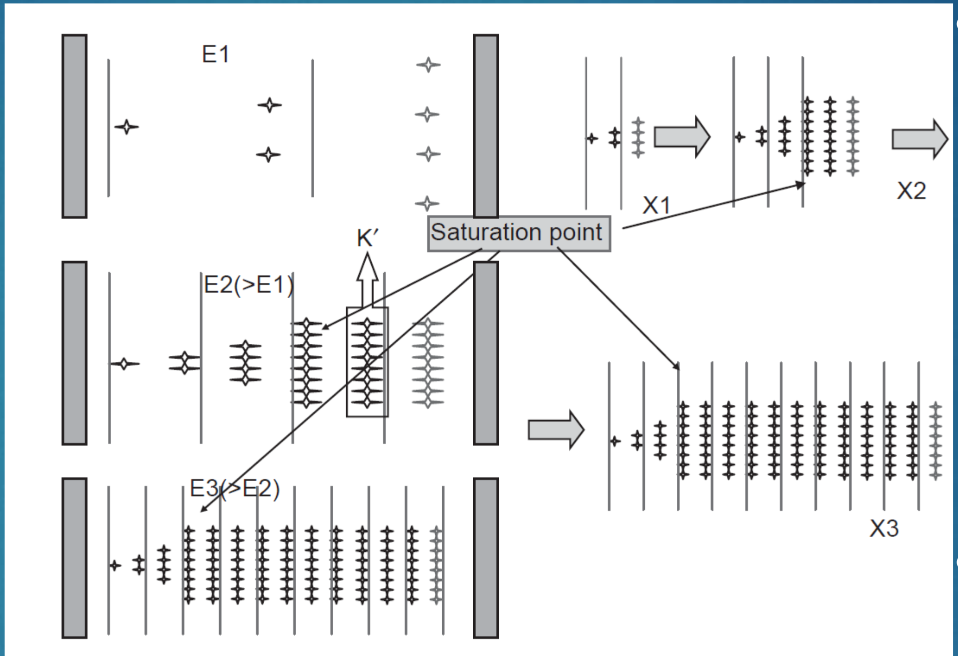

- As a function of the space

$$\frac{\mathrm{d}Q_{\mathrm{act}}}{\mathrm{d}x} = \alpha Q_{\mathrm{act}}\left(1 - \frac{Q_{\mathrm{act}}}{K}\right)$$

$$Q_{\mathrm{act}}(x) = \frac{K}{1 + \mathrm{e}^{-\alpha(x - x_0)}}$$

$$Q_{\mathrm{act}}(x = 0) = Q_0$$

- α is the Townsend coefficient
- The total collected charge as a function of the space

$$Q_{\mathrm{tot}}(x) = Q_0 + \int_0^x Q_{\mathrm{act}}(x')\alpha\,\mathrm{d}x' = Q_0 + K \ln \frac{1 + \mathrm{e}^{\alpha(x - x_0)}}{1 + \mathrm{e}^{-\alpha x_0}}.$$

The Qtot to Qprompt ratio

- Qtot it the “price” to pay in charge to deliver a signal Qprompt (the charge induced by the moving electrons)
- Starting from the example of the ionization chamber, is easy to demonstrate that a purely exponential avalanche has a Qtot to Qprompt ratio proportional to αg where g is the gas volume thickness with α=20 it is certainly a large constant
- In the streamer case, it is also easy to show that the ratio is 2
- One expects an intermediate situation for the saturated avalanche, which is function of the saturation
- It is necessary to introduce the attachment coefficient transforming an electron in a negative ion (removed)

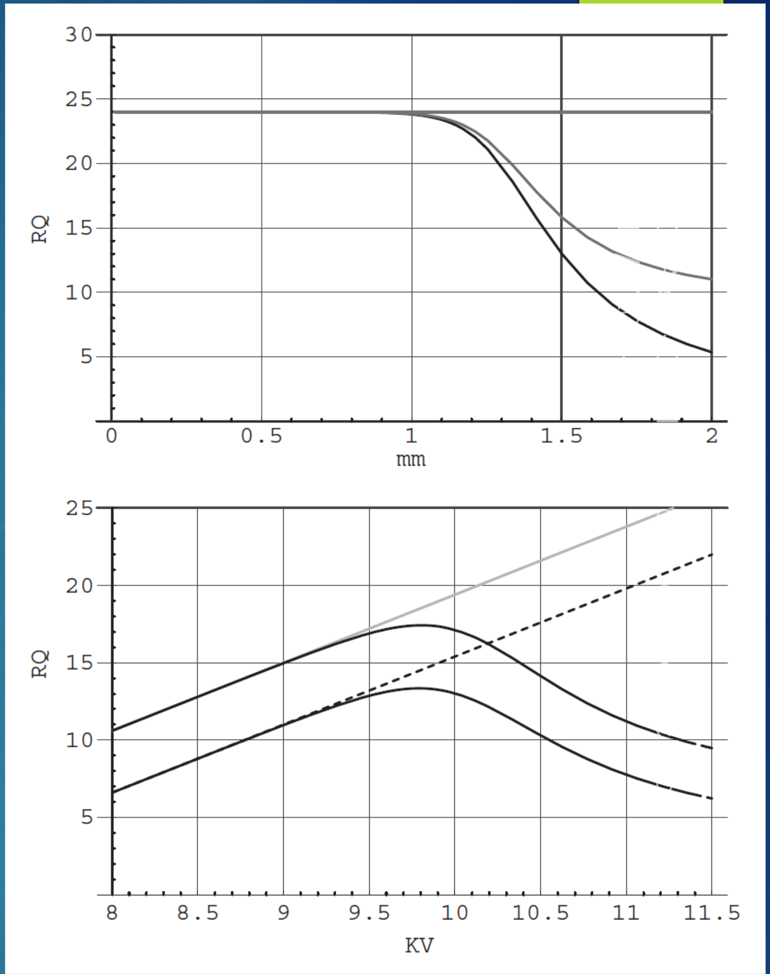

$$\frac{\mathrm{d}Q_{\mathrm{free}}}{\mathrm{d}x} = \alpha Q_{\mathrm{act}} - \gamma Q_{\mathrm{free}}$$

$$Q_{\mathrm{prompt}} = \frac{1}{g} \int_0^g Q_{\mathrm{free}}(x)\,\mathrm{d}x$$

$$R_Q = \frac{Q_{\mathrm{tot}}}{Q_{\mathrm{prompt}}} = g\,\frac{\int_0^g Q_{\mathrm{act}}(x)\alpha\,\mathrm{d}x}{\int_0^g Q_{\mathrm{free}}(x)\,\mathrm{d}x}$$

For a completely saturated avalanche, i.e. $x \gg x_0 \xrightarrow{\text{yields}} Q_{tot}(x) \cong K \propto x$ and R_Q is found to decrease down to the limit value 2 (for the case $\gamma = 0$ $Q_{free} = Q_{tot}$).